

# Massive mobilization of toxic elements from an intact rock glacier in the Central Eastern Alps: ~~insights into ice melt dynamics~~

Hoda Moradi<sup>1,\*</sup>, Gerhard Furrer<sup>2</sup>, Michael Margreth<sup>3</sup>, David Mair<sup>1</sup>, Christoph Wanner<sup>1</sup>

<sup>1</sup>Institute of Geological Sciences, Department of Earth Sciences, University of Bern, Baltzerstrasse 3, CH-3012 Bern, Switzerland

<sup>2</sup>Institute of Biochemistry and Pollutant Dynamics (IBP), Department of Environmental Systems Science, ETH Zurich, CH-8092 Zurich, Switzerland

<sup>3</sup>Swiss Federal Institute for Forest, Snow and Landscape Research WSL, Mountain Hydrology and Mass Movements, Zürichstrasse 111, CH-8903 Birmensdorf, Switzerland

10 \*Correspondence to: Hoda Moradi ([hoda.moradi@unibe.ch](mailto:hoda.moradi@unibe.ch))

**Abstract.** In the Central Eastern Alps, an increasing number of high-altitude streams draining ice-rich permafrost display high concentrations of toxic solutes such as Al, F, Mn, and Ni that may strongly exceed drinking water limits. To obtain novel insights into the causes for the mobilization of toxic solutes and to assess the environmental hazard, here we present a two-year dataset (2021, 2022) of monitoring a high-alpine stream originating from an intact rock glacier located in Eastern Switzerland. The monitoring includes monthly sampling and discharge measurements as well as continuous tracking of the geogenic fluxes of toxic solutes using a pressure and conductivity probe. Our monitoring revealed high annual fluxes of up to 10 t per year with strong seasonal variations. In particular, the fluxes were highest during the warm summer months and show strong correlations with hydraulic events such as snowmelt and heavy rainfall. These correlations likely occur because the mobilization of toxic solutes reflects the last step of a complicate sequence of coupled processes including (i) the oxidation of sulfides producing sulfuric acid and promoting the dissolution of solutes from the host rock, (ii) temporal storage and long-term enrichment of the dissolved solutes in rock glacier ice, and (iii) their final hydraulic mobilization during climate-change induced accelerated degradation of rock glaciers. In the studied catchment, the concentrations of toxic solutes strongly exceed the drinking water limits down to an altitude of 1900 m a.s.l. This forms a significant hazard for the farmers and their products using the catchment in summer, while the hazard for larger streams in populated areas further downstream is considered limited. Since the fluxes of toxic solutes downstream of rock glaciers essentially reflect their final hydraulic mobilization from the solute-enriched rock glacier ice, we hypothesize that flux measurements may serve as a novel environmental tracer to study permafrost degradation.

## 1 Introduction

Rock glaciers form valuable long-term freshwater resources and are thus important for high-alpine water budgets (Jones et al., 2018; Wagner et al., 2021). Rock glaciers are distinct sediment bodies in the landscape, often tongue-shaped and present in high alpine environments that comprise poorly sorted and angular rock debris, and ice. Based on their ice content and

movement behavior, rock glaciers are categorized into three groups: i) active rock glaciers, which contain ice and show movement; ii) inactive rock glaciers, which retain ice but no longer move; and iii) relict rock glaciers, which neither contain ice nor display movement. Both active and inactive rock glaciers are collectively referred to as intact (Haeberli, 1985; Barsch, 1996; Jones et al., 2019). ~~They can~~ Active rock glacier move as a result of the deformation of internal ice, leading to a gravity-driven creep of these landforms (Jones et al., 2019; Giardino and Vitek, 1988; Barsch, 1996). The internal structure of active rock glaciers is composed of ~~two~~ three fundamental components. Firstly, there is the active layer ~~(AL)~~, which is a seasonally frozen debris layer, usually several decimeters to a few meters thick (Humlum, 1997). Secondly, beneath the active layer, there is a core of ice-supersaturated debris (non-glacial) and pure ice (glacial), as described by Ballantyne (2018). ~~If all ice has melted, rock glaciers stop to creep and are classified as relict (Jones et al., 2018, 2019).~~ Thirdly, an unfrozen, fine-grained layer typically occurs at the base of rock glaciers. This base layer acts as aquifer and thus strongly contributes to the high storage capacity of rock glaciers (Hayashi, 2020; Harrington et al., 2018). The current inventory of global rock glacier water volume equivalent has been recently estimated to be  $83.2 \pm 16.64$  Gt, representing about 2 % of the water volume equivalents stored in glaciers when excluding high-latitude cold regions (Jones et al., 2018). Because rock glaciers are more resilient to climatic fluctuations than mountain glaciers, the rapid retreat of the latter will increase the role of rock glaciers as freshwater storage with ongoing climate change (Jones et al., 2019 and references therein; Li et al., 2024). This is supported by the observation that in arid regions like North Asia, rock glaciers store up to 4% of the water equivalent found in mountain glaciers with only few mountain glaciers such as North Asia, the ratio between water equivalents stored in rock glaciers and those stored in glacier is up to 4% (Jones et al., 2018). A study in Austria suggested an even higher ratio of about 1:12 (8.3%) for rock glacier to glacier ice A regional study conducted in Austria even proposed a water equivalent ratio of about 1:12 (8.3 %) for rock glacier versus glacier ice (Wagner et al., 2021a). ~~To evaluate the contribution of rock glaciers to the hydrological system, it is essential to measure the discharge of meltwater into the hydrological system (Mark and Mckenzie, 2007).~~

~~Despite the increasing importance of intact rock glaciers for the hydrology of high mountainous areas, little is known to date regarding their ice melt export in rock glaciers; in particular, how much this contributiones to the discharge of mountainous streams. Geophysical methods including ground penetrating radar (GPR), electrical resistivity tomography (ERT), and refraction seismic tomography (RST) are typically applied to elucidate the internal structures of rock glaciers (Hauck, 2013; and references therein). For instance, Mewes et al. (2017) combined ERT and RST inversions to visualize the summer ice loss in the Bee de Bosson rock glacier in Switzerland. Furthermore, Hauck et al. (2011) verified the effectiveness of utilizing tomographic electrical and seismic imaging techniques to quantify contributions of ice, water, and air in permafrost regions and identify solid bedrock. None of these geophysical methods, however, allows to estimate contribution of meltwater from rock glacier to the downhill mountainous streams during ice melt season. Nevertheless, Krainer et al. (2015) estimated a yearly ice volume loss of  $10,000 \text{ m}^3$  for the Lazaun rock glacier in Southern Tyrol, Italy, corresponding to the uppermost 10 cm of the frozen rock glacier core, using differential GPS measurements combined with information obtained from two drill~~

cores of this rock glacier. Subsequently, they compared this volume to the discharge continuously measured downstream of a spring discharging from the rock glacier. This resulted in an estimated yearly average contribution of ice melt on the discharge of  $0.6 \text{ L s}^{-1}$ , which corresponded to about 2 % of the discharge from the entire rock glacier. The apparent little contribution of ice melt from the rock glacier to the total discharge demonstrates that these discharges represent a mixture of various water sources including rainwater, snowmelt, ice melt, and longer stored groundwater (Jones et al., 2019; Wagner et al., 2021b). To differentiate between the different water sources, a significant number of hydrological studies have continuously monitored rock glacier springs by performing measurements of parameters including discharge, electrical conductivity, stable isotopes (i.e.  $\delta^{18}\text{O}$ ,  $\delta^2\text{H}$  values), and dissolved solutes (Williams et al., 2006; Krainer et al., 2007; Brighenti et al., 2021; Wagner et al., 2021a,b; Munroe and Handwerker, 2023). Most of these studies provided estimates for seasonally variable relative contributions of the different discharge components. However, since all of them utilized stable isotope data, the rather strong seasonal variations of snowmelt and rainwater  $\delta^{18}\text{O}$  and  $\delta^2\text{H}$  values form a significant challenge for quantifying ice melt export rates using stable isotope data (Wanner et al., 2023b). Moreover, in case of the “Innere Ögrube” rock glacier, Ötztal Alps, Austria, the discharge from the rock glacier also contains a contribution from an uphill mountain glacier, which could not be differentiated from the ice melt being exported in the rock glacier (Wagner et al., 2021a).

While rock glaciers may become more important for the drinking water supply of high-alpine regions (Jones et al., 2019; Wagner et al., 2020; 2021b), the anticipated increase in ice melt export rates may cause serious environmental challenges. In regions with sulfide-bearing (e.g., pyrite) and carbonate-free bedrock, such as in the Central Eastern Alps, an increasing number of high-altitude streams originating from intact rock glaciers display high concentrations of toxic solutes such as aluminum, nickel, manganese, and fluoride that may strongly exceed drinking water limits (Thies et al., 2007; Ilyashuk et al., 2014; Wanner et al., 2023). Outside the European Alps, the same is observed, for instance, downstream of permafrost areas in the Pyrenees in Spain (Zarroca et al., 2021) or the Rocky Mountains in the US (Todd et al., 2012). Moreover, elevated solute concentrations have also been observed downstream of ice glaciers (e.g., Fortner et al., 2011; Dold et al., 2013). Most recently, highly acidic conditions and high solute concentrations have been additionally described in seeps draining high-latitude permafrost areas in Alaska, affecting the water quality of streams on the regional scale (O’Donnell et al., 2024). It follows that elevated solute concentrations in water draining from permafrost areas are a global phenomenon (Colombo et al., 2018; Brighenti et al., 2019). High concentrations of toxic solutes impact water quality, thereby affecting humans, plants, and animals. (Vergilio et al., 2021; Shaw and Tomljenovic, 2013; Exley, 2016). In particular, they affect fish species and the biodiversity in the affected streams. (Muniz, 1990; Brighenti et al., 2019; O’Donnell et al., 2024). The adverse water quality of rock glacier springs is often caused by acid rock drainage (ARD), where the weathering of sulfide-bearing minerals such as pyrite produces sulfuric acid and, therefore, promotes the leaching of toxic elements from the crystalline host rocks (Todd et al., 2012; Ilyashuk et al., 2014, Wanner et al., 2018; 2023a). Recently, Wanner et al. (2023) have hypothesized that the increased mobilization of toxic solutes from intact rock glaciers observed today additionally requires their temporal storage

100 and long-term enrichment in the frozen rock glacier core. This is because the oxidation of pyrite and other sulfuric acid  
generating sulfides is kinetically limited (Williamson and Rimstidt, 1994) and the pyrite content of the studied rock glaciers  
affected by ARD is rather low (Wanner et al., 2023). This hypothesis is consistent with high concentrations of the same  
elements (e.g., Ni, Zn, Mn) in frozen rock glacier cores as those showing high concentrations in rock glacier springs (Nickus  
105 et al., 2023). Moreover, it implies that the climate-change-induced accelerated melting of rock glaciers causes a quick and  
focused export in summer when production rates from ice melt are high, and that solute fluxes will increase in the near  
future.

To verify these storage and enrichment hypothesis and to assess the consequences of accelerated rock glacier degradation on  
the water quality of high alpine streams, we have initiated detailed monitoring of a high alpine catchment in the Central  
110 Eastern Alps in Switzerland. Here, we present monitoring results for the years 2021 and 2022. In contrast to most previous  
rock glacier monitoring studies focusing on recording solute concentrations (e.g., Williams et al., 2006; Krainer et al., 2007;  
Brighenti et al., 2021; Wagner et al., 2021a, b; Munroe and Handwerger, 2023), our aim was to systematically record solute  
fluxes being exported from the intact rock glacier at the origin of the study catchment. The idea behind this approach is that  
unlike solute concentrations, fluxes are not affected by an unknown degree of dilution caused by snowmelt and rainwater.  
115 Consequently, the collected data provide novel insights into the coupled thermal-hydraulic-chemical processes controlling  
the discharge and water quality of high-alpine streams originating from intact rock glaciers. In the context of global  
warming, this information is key to assess the environmental hazard caused by ARD in ice-rich permafrost systems such as  
rock glaciers.

To test this approach and to further assess the consequences of accelerated rock glacier melt on the stream water quality, we  
120 have initiated a detailed monitoring of a high alpine catchment in the Central Eastern Alps in Switzerland. Here we present  
monitoring results for the years 2021 and 2022 with a particular focus on toxic element solute fluxes being exported from the  
intact rock glacier at the origin of the catchment. The strong seasonality of the fluxes with extreme values exceeding 100 kg  
per day during the hot summer months confirm the close link between element fluxes and ice melt export rates.  
Consequently, the collected data provide novel insights on the coupled thermal-hydraulic-chemical processes controlling the  
125 discharge and water quality of high alpine streams originating from intact rock glaciers. In the context of global warming,  
this information is key to assess the role of intact rock glaciers for the future water budget in high alpine streams as well as  
the associated environmental hazard caused by ARD in such systems.

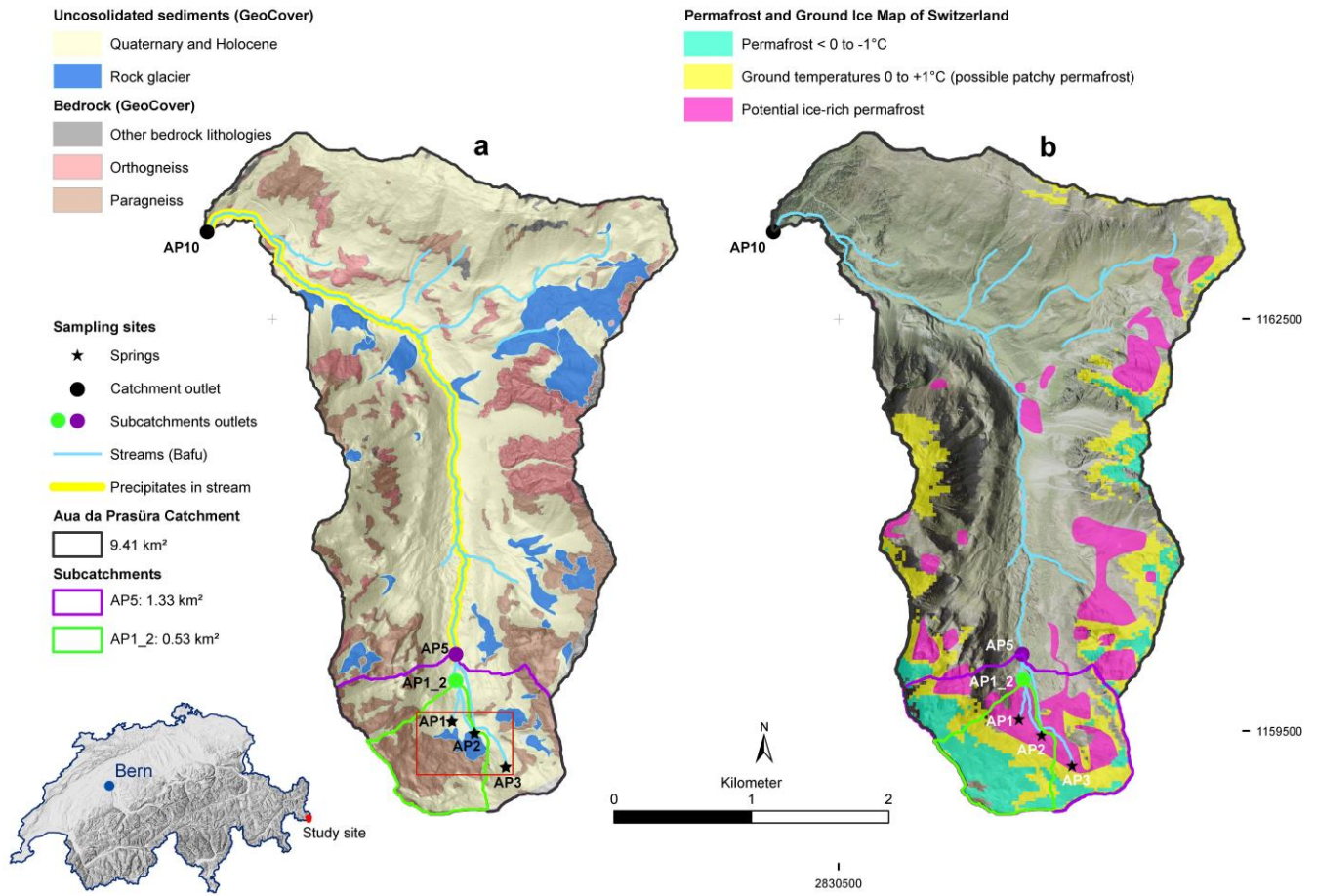
## 2 Site description

Our flux monitoring is set up along the Aua da Prasüra mountain stream located in the Val Costainas valley in the Eastern  
130 part of Switzerland, close to the Swiss-Italian border (Fig. 1a). The monitored catchment encompasses a remote area of 9.41  
km<sup>2</sup> at an altitude ranging from 1900 to 2800 m a.s.l. with no mining and almost no other anthropogenic activities apart from

alpine livestock farming during summertime. Geologically, the area is part of the crystalline basement of the Austroalpine nappes (Schmid et al., 2004). These basement nappes are devoid of carbonate rocks as well as pyrite-bearing and mostly consist of mica-rich, strongly weathered paragneiss and quartz-rich orthogneiss (Swisstopo, 2024a; Schmid, 1973).  
135 Quaternary sediment deposits, consisting of material from these units, such as moraines and alluvial cones, cover a substantial part of the study area. In addition, the catchment is free of ice glaciers, and both intact and relict rock glaciers are frequently found in it. The Aua da Prasüra stream itself originates from three springs (AP1, AP2, and AP3, Fig. 1), discharging from an ice-rich permafrost zone (Fig. 1b) with the typical morphology of an intact rock glacier (Fig. 2). Based on the geological map of the catchment (Fig. 1a) as well as a high-resolution digital elevation model resulting from UAV  
140 (uncrewed aerial vehicle) imagery (Fig. 2), the surface area of the rock glacier at the origin of the stream is approximately 40,000 m<sup>2</sup> (Fig. 2). A photo of the entire valley is provided in the Supplement (Fig. S2).

As described previously in Wanner et al., (2023), the three rock glacier springs show a typical acid rock drainage (ARD) signature with pH values as low as 5.0; and concentrations of Al, F, Mn, and Ni exceeding the corresponding drinking water  
145 limits by up to 2 orders of magnitude. The discharge from the rock glacier is highest at the spring located at the lowest elevation (AP1, 2660 m a.s.l.). While this spring is constantly discharging water, the two others, located at 2700 (AP2) and 2770 (AP3) m a.s.l., respectively, fell dry in late summer during both monitoring years. Downstream of sampling location AP5 the pH and temperature increases to values above 5.5 and 5 °C, respectively, resulting in the precipitation of nanocrystalline basaluminite ( $\text{Al}_4\text{OH}_{10}(\text{SO}_4) \times (\text{H}_2\text{O})_5$ ) because of its strong pH- and temperature-dependent solubility  
150 (Wanner et al., 2018, 2023). The precipitation is visible as white coatings on the bedload of the stream (Fig. S1, Supplement) until the outlet of the catchment, which is about 5 km downstream at an altitude of 1890 m a.s.l. at sampling location AP10 (Fig. 1a). Based on historical aerial photographs, basaluminite precipitation only occurs since the Year 2000 (Wanner et al., 2023). This observation serves as a strong indicator of a significant decline in the water quality of the monitored stream over the past 30 years.

# Val Costainas



## Val Costainas

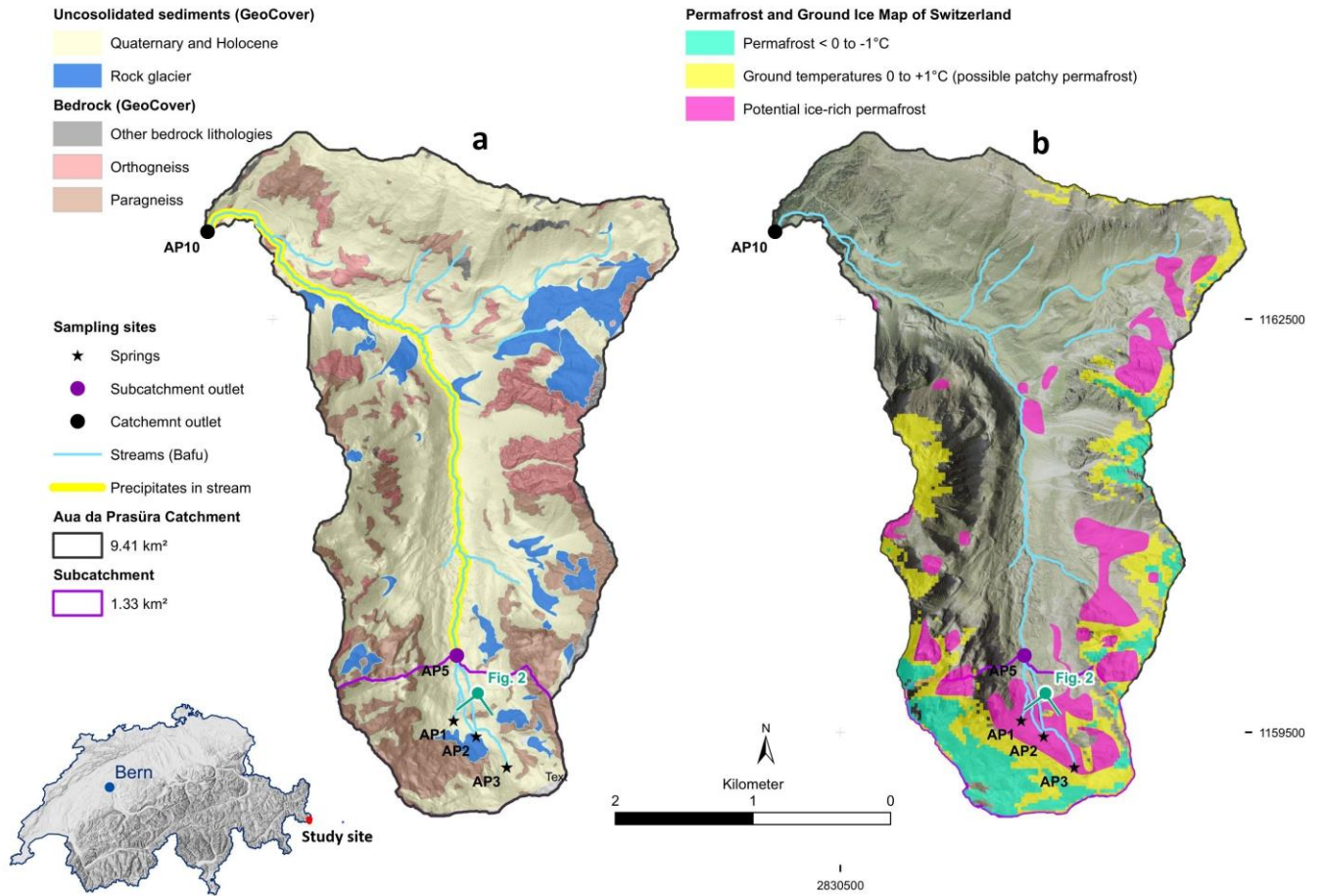
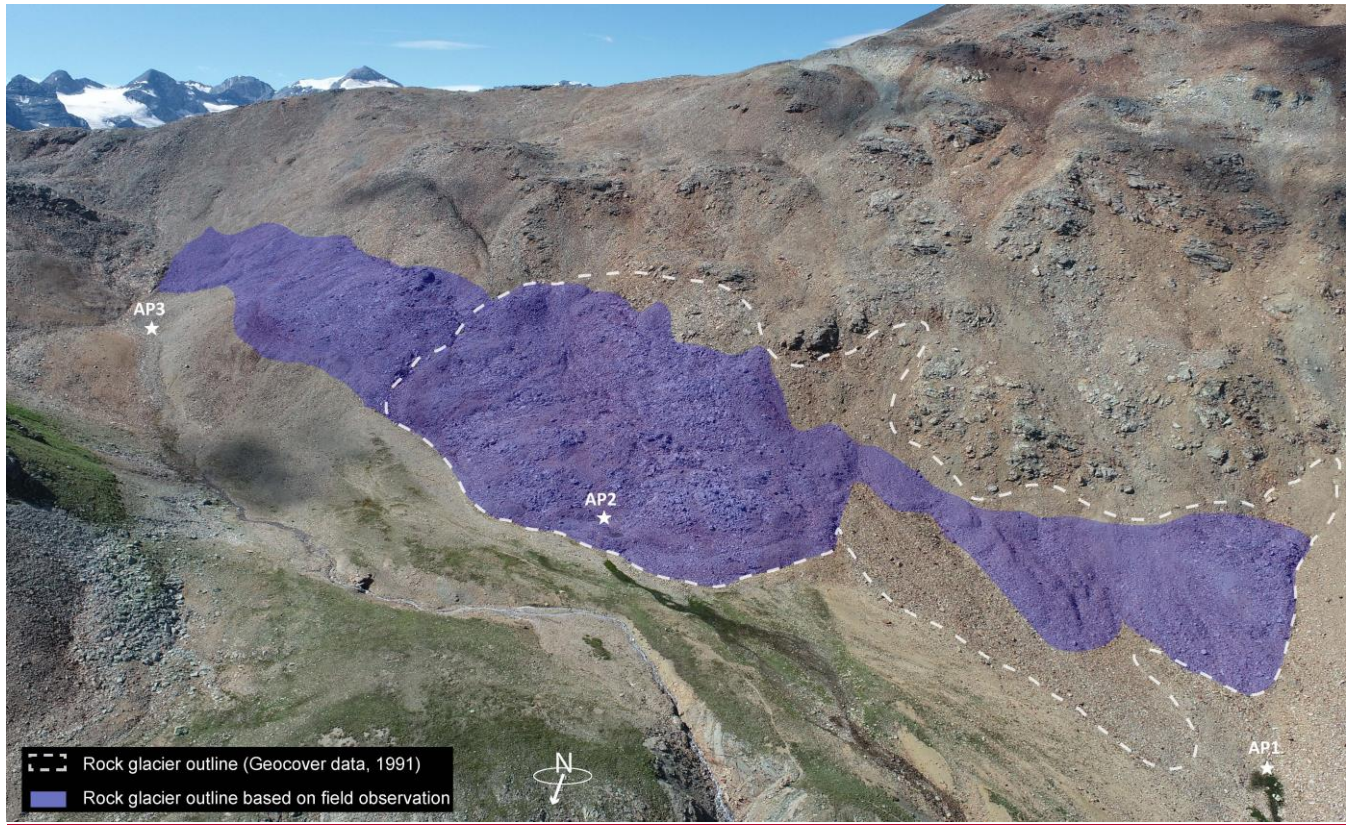


Figure 1: Val Costainas. (a) Geological map modified from the GeoCover dataset, map sheet Sta Maria-Münstair –from the Federal Office of Topography and swisstopo (Swisstopo, 2024b) based on field observations, and (b) permafrost and ground ice map of the Aua da Prasüra catchment (Kenner et al., 2019). The star symbols refer to the locations of the three rock glacier springs at the origin of the catchment (AP1, AP2, and AP3). The purple and black filled circles refer to the two sampling locations downstream of the rock glacier (AP5, AP10), and the convergence point of AP1 and AP2, which is called AP1 2 (green). The green circle with the two tips red rectangle illustrates contains shows the location and direction of the UAV for taking the photograph of the studied rock glacier shown in Figure 2. The section of the stream with white-coated bedload coatings (i.e. basaluminite, Fig. S1, Supplement) is highlighted in yellow. Basemaps: SwissAlti3D digital elevation model and SWISSIMAGE (© swisstopo).







170 **Figure 2: UAV (uncrewed aerial vehicle) photograph of the entire rock glacier with the three rock glacier springs AP1, AP2, and AP3. The dashed line represents the rock glacier outline based on the GeoCover data shown on Figure 1a (Swisstopo, 2024b). The blue polygon shows our interpretation of the current rock glacier outline based on field observations. The photograph was captured on July 6, 2022.**

### 3 Methods

175 The main aim of our monitoring is to continuously track the fluxes of toxic solutes being transported in the Aua da Prasūra stream. To relate these to the exported fluxes from the intact rock glacier at the origin of the stream, we chose two main monitoring locations: (i), the merging point of the three rock glacier springs at location AP5, and (ii) -AP10, located about 5 km downstream of the rock glacier (Fig. 1). With a catchment size of 1.33 km<sup>2</sup>, location AP5 corresponds to 14 % of the catchment size monitored at AP10 (catchment area = 9.41 km<sup>2</sup>). The AP5 subcatchment includes the entire rock glacier shown in Figure 2 as well as other ice-rich permafrost areas. To estimate how much of the fluxes measured at AP5 originate  
180 from the actual rock glacier, solute fluxes were also periodically measured at AP1\_2, located approximately 200 meters downstream of AP1. Here the springs from AP1 and AP2 merge, and are not affected by AP3 or most of the ice-rich permafrost area outside of the main rock glacier shown in Figure 2.

185 The monitoring includes the collection and analysis of streamwater samples, as well as manual and automated measurements of the stream discharges, as detailed below. Because of the presence of large rock boulders, the seasonally low discharge, and the potential relevance of hidden subsurface flow, reliable discharge and flux measurements at the three rock glacier springs are impossible (AP1, AP2, and AP3, Fig. 1).

### 190 **3.1 Sampling of streamwater**

Streamwater samples were collected from ~~six~~five different locations: AP1, AP2, AP3, AP1 2, AP5, and AP10 (Fig. 1). Sampling took place between May and October of 2021 and 2022, with different sampling intervals. At the most downstream and best accessible location at AP10, samples were collected biweekly ~~and also~~ almost outside the May to October throughout the whole year period. In the source region, AP1, AP1 2, and AP5, corresponding to the rock glacier spring with the highest discharge and merging points of the rock glacier springs, respectively, sampling was carried out approximately every 1.5 months. The two additional rock glacier springs (AP2, AP3) could only be sampled sporadically because they usually fall dry after the termination of the snowmelt in late summer. For all samples, pH, electrical conductivity (EC), and water temperature were measured on-site using Hamilton electrodes with Knick Portamess-913 field instruments. In addition, samples were filtered on-site using 0.2 µm filters and stored in polyethylene bottles. For the analyses of major cations and trace elements, one aliquot per sample was acidified using ~~one drop of~~ a 30 % HNO<sub>3</sub> solution until the sample had a pH between 2 and 3. All samples were stored at 4 °C prior to analysis.

### 200 **3.2 Discharge measurements using tracer-dilution**

At the three discharge monitoring sites (AP1 2, AP5, and AP10), the discharge of the stream was measured manually approximately every 1.5 months between May and October of 2021 and 2022. At AP10, discharge measurements were additionally performed in early spring (March-April). These measurements were carried out with the Sommer TQ-S Tracer System using the well-established tracer-dilution method with NaCl as tracer (e.g., Calkins and Dunne, 1970; Day, 1977; Leibundgut et al., 2009) and an uncertainty of ±5 %. Additional –details of the tracer-discharge measurements are provided in the Supplement (Section S1). ~~The Tracer System consists of two electrical conductivity probes connected via Bluetooth to the Software TQ Commander. For each site, the probes were calibrated with streamwater samples, allowing the calculation of NaCl concentrations based on electrical conductivity values (calculation is executed automatically by the software). When a fixed quantity of NaCl is added upstream, the system automatically quantifies the discharge based on the NaCl concentrations registered at the measurement site (integral of concentration curves). For each discharge quantification, we executed two measurements by using different amounts of salt, resulting in four measurements in total. The reported discharge values constitute the average of these four measurements. Based on the spread of the measurements, the~~

215 ~~uncertainty of the discharge quantification was well within  $\pm 5\%$ , which is consistent with the maximum measurement~~  
~~uncertainty estimated by the producer company (Sommer). In general, the uncertainty of discharge measurements using the~~  
~~salt dilution method depends on calibration, the amount of used salt and on the measurement setup, i.e. the length of mixing~~  
~~section. The better the salty water is mixed with the stream water, the higher the accuracy of measured discharge values.~~  
~~These aspects were taken into account during the measurements.~~

220

### 3.3 Automatic water table and electric conductivity measurements

At the AP10 location, the Canton of Graubünden operates a combined water table, temperature, and conductivity probe. The  
probe takes a measurement of these parameters every ten minutes and the data are published online in real time (ANU,  
2023). During wintertime, the discharge of the stream is very low, and the stream is periodically covered by snow and an ice  
225 layer, which render the readings of the probe unreliable. With the beginning of the snowmelt season in spring, the discharge  
increases, and the data recorded by the probe becomes more reliable. Based on our observations, we consider the recorded  
data from May to October to be reliable, and we exclusively utilize these measurements for analysis.

~~The information on water table was used for discharge estimation (S2 and S3, Supplement) and the EC values were used~~  
~~Nevertheless, even in summertime, loss of data occurred. To overcome this problem, different approaches were applied. In~~  
230 ~~the event of water table data loss, the data were handled differently based on the circumstances. In regular situations without~~  
~~any notable meteorological events, a linear interpolation method was employed to reconstruct the missing data. If the data~~  
~~loss occurred immediately after a precipitation event, a typical recession curve equation (Maillet, 1905) was used:~~

$$Q_t = Q_0 e^{-\alpha t} \quad (1)$$

235 
$$\alpha = \frac{\log Q_0 - \log Q_t}{0.4343 t} \quad (2)$$

Where  $Q_t$  is the discharge at time  $t$  in  $\text{m}^3 \cdot \text{s}^{-1}$ ,  $Q_0$  is the discharge at time 0 in  $\text{m}^3 \cdot \text{s}^{-1}$ ,  $t$  is the time between  $Q_0$  and  $Q_t$  in  
seconds, and  $\alpha$  is discharge coefficient, collected after the data recording had been resumed. A slightly different approach  
was used in the event of electrical conductivity measurement problems to reconstruct for the missing data. Since we used  
240 these data to estimated solute concentrations (see below), the chemical analyses of the biweekly samples were used to ensure  
the continuity of the concentration estimates via linear interpolation during such events. Based on the comparison with  
manual discharge and conductivity measurements, the uncertainty of the automated water table and electric conductivity  
measurements were estimated to  $\pm 1$  cm and  $\pm 5\%$ , respectively.

### 3.4 Analytical methods

#### 245 3.4.1 Water analysis

Concentrations of major cations and anions,  $\text{Na}^+$ ,  $\text{K}^+$ ,  $\text{Ca}^{2+}$ ,  $\text{Mg}^{2+}$ ,  $\text{NH}_4^+$ ,  $\text{F}^-$ ,  $\text{Cl}^-$ ,  $\text{Br}^-$ ,  $\text{NO}_3^-$ ,  $\text{SO}_4^{2-}$ , of the streamwater samples were measured by ion chromatography (IC) at the University of Bern using a Metrohm 850 system with a detection limit of  $0.1 \text{ mg L}^{-1}$  for cations and  $0.016 \text{ mg L}^{-1}$  for anions. Total inorganic and organic carbon concentrations were determined using a TIC/TOC analyzer (Analytik Jena multi N/C 2100S) with detection limits of  $0.1 \text{ mg L}^{-1}$  for inorganic and  $0.5 \text{ mg L}^{-1}$  for organic carbon. Inductively coupled plasma optical emission spectroscopy (ICP-OES) with a Varian 720-ES ICP spectrometer was used to determine aqueous concentrations of Al, Ba, Cu, Fe, Mn, Ni, Zn, Si, Sr, Pb and Cd. The detection limit was  $1 \text{ } \mu\text{g L}^{-1}$  for Ba, Mn, Sr and Zn,  $3 \text{ } \mu\text{g L}^{-1}$  for Al and Si,  $5 \text{ } \mu\text{g L}^{-1}$  for Fe, Ni, Cd and Cu, and  $20 \text{ } \mu\text{g L}^{-1}$  for Pb. Concentrations of As were determined by atomic adsorption spectroscopy (AAS) using a ContraA 700 (Analytik Jena) with a detection limit of  $4 \text{ } \mu\text{g L}^{-1}$ . The analytical error of all these measurements was within  $\pm 5\%$ .

#### 255 3.5 Determination of fluxes

At the three discharge monitoring sites (AP1 2, AP5, and AP10), discharge measurements were carried out right after collecting streamwater samples. Accordingly, the fluxes of solutes (e.g., in  $\text{mg s}^{-1}$ ) correspond to the product of their concentrations (e.g., in  $\text{mg L}^{-1}$ ) and the measured discharge (e.g., in  $\text{L s}^{-1}$ ). Between May and October of 2021 and 2022, our data thus allow determining solute fluxes every 1.5 months. In addition to these sporadic flux determinations, we have continuously estimated the fluxes of solutes at the downstream location (AP10) using the continuous water table and electrical conductivity data collected by the installed probe. To do so, water table measurements were correlated with discharge measurements to obtain a discharge-water table relationship (rating curve) allowing to continuously determine the discharge. Likewise, the electrical conductivity measurements were correlated with solute concentrations measured on the biweekly water samples to establish a conductivity-concentration relationship for the continuous determination of solute concentrations. In the event of probe malfunctioning, the missing discharge and concentration data at AP 10 were reconstructed as detailed in Section S2 of the Supplement. The product of ~~these two determinations~~ discharge and concentration resulted in daily averages of solute fluxes. In this study, we focus on the fluxes of Al, F<sup>-</sup>, Zn, Mn, and Ni because these solutes are of the highest environmental concern in streams affected by ARD in the Central Eastern Alps (Wanner et al., 2023). Taking into account the errors of the individual measurements (discharge, electrical conductivity, element concentrations) used for the continuous flux estimations, the uncertainty was estimated to be within  $\pm 10 \%$ .

#### 3.6 Snow height, precipitation and temperature data

Snow height values for 2021 and 2022 were obtained from the Murtaröl snow station, located approximately 15 km Northwest of AP10 at an elevation of 2359 m a.s.l. (SLF, 2023). Similarly, the precipitation and atmospheric temperature

275 data for both years were acquired from the Santa Maria weather station, which is about 6.5 km north of AP10 at an altitude of 1388 m a.s.l. (MeteoSwiss, 2023).

## 4 Results

### 4.1 Discharge measurements

#### 4.1.1. ~~I~~ntermittent discharge measurements at AP1 2, AP5 and AP10

280 The intermittent discharge measurements at the ~~threetwo~~ monitoring locations showed strong seasonal variations (Table 1). The highest values above 50 L s<sup>-1</sup> (AP1 2), 200 L s<sup>-1</sup> (AP5) and 1000 L s<sup>-1</sup> (AP10) were measured during snowmelt in late spring or early summer (May-July). At AP10, the lowest discharge (< 70 L s<sup>-1</sup>) was recorded in early spring (Mar-Apr) when the winter recession of discharge ended before the snowmelt period started. Owing to the high altitude, no sampling was possible at AP1 2 and AP5 at this time. Accordingly, the lowest discharge ~~was measured at AP1 2 (<15 L s<sup>-1</sup>) and AP5 (<30 L s<sup>-1</sup>) were measured~~ in early fall in both monitoring years.

285 In addition to the seasonal discharge variations, the ratio of the discharge at the upstream (AP1 2 and AP5) and downstream (AP10) monitoring sites strongly varied. For AP5, this proportion is provided in Table 1. With the exception of the peak snowmelt period captured on 10 June 2021, the discharge at AP5 relative to that at AP10 was always higher than the 14 % expected from the difference in the corresponding catchment areas. In both monitoring years, the ratio peaked with values above 30 % right after the termination of the snowmelt in early July and, hence, up to 3 times higher than expected from the two catchment sizes. During low discharge conditions in fall, the relative discharge at AP5 was still slightly below 20 % and hence at least 1.3 times higher than expected from the area of the two catchments. The continuous discharge data for the downstream location AP10 obtained from the discharge-water table relationship (Section S3, Supplement) are presented with the seasonal flux estimates below.

Table 1: Discharge measurements at the ~~three~~**two** monitoring locations and relative discharge contribution of the upstream catchment at AP5 on the discharge of the entire catchment at AP10 (Fig. 1). Also the relative discharge contribution AP5/AP10 normalized by the ratio of the two catchment areas (AP5: 1.33 km<sup>2</sup>; AP10: 9.41 km<sup>2</sup>) is shown, ~~to illustrate that the discharge from the upstream catchment and hence the rock glacier at the source of the stream is disproportionately high.~~

Date	Discharge at AP1 (L s <sup>-1</sup> )	Discharge at AP5 (L s <sup>-1</sup> )	Discharge at AP10 (L s <sup>-1</sup> )	Relative discharge contribution AP5/AP10 (%)	Ratio between relative discharge contribution AP5/AP10 and ratio of the two catchment areas (1.33/9.41)
<u>23 March 2021</u>	-	-	<u>53</u>	-	-
<u>10 June 2021</u>	-	<u>153</u>	<u>1116</u>	<u>14</u>	<u>1</u>
<u>08 July 2021</u>	-	<u>269</u>	<u>629</u>	<u>43</u>	<u>3</u>
<u>18 August 2021</u>	<u>31</u>	<u>58</u>	<u>410</u>	<u>14</u>	<u>1</u>
<u>22 September 2021</u>	<u>14</u>	<u>26</u>	<u>136</u>	<u>19</u>	<u>1.4</u>
<u>21 October 2021</u>	<u>18</u>	<u>34</u>	<u>182</u>	<u>18</u>	<u>1.3</u>
<u>02 April 2021</u>	-	-	<u>64</u>	-	-
<u>20 May 2021</u>	-	-	<u>733</u>	-	-
<u>05 July 2021</u>	<u>52</u>	<u>91</u>	<u>306</u>	<u>30</u>	<u>2.1</u>
<u>13 August 2021</u>	<u>28</u>	<u>47</u>	<u>203</u>	<u>23</u>	<u>1.6</u>
<u>11 October 2021</u>	<u>13</u>	<u>27</u>	<u>140</u>	<u>19</u>	<u>1.4</u>

Date	Discharge at AP5 (L s <sup>-1</sup> )	Discharge at AP10 (L s <sup>-1</sup> )	Relative discharge contribution AP5/AP10 (%)	Relative discharge contribution AP5/AP10 normalized by the ratio of the two catchment areas (1.33/9.41)
<del>23 March 2021</del>	<del>n.m.</del>	<del>53</del>	<del>-</del>	<del>-</del>
<del>10 June 2021</del>	<del>153</del>	<del>1116</del>	<del>14</del>	<del>1</del>
<del>8 July 2021</del>	<del>269</del>	<del>629</del>	<del>43</del>	<del>3</del>
<del>18 August 2021</del>	<del>58</del>	<del>410</del>	<del>14</del>	<del>1</del>
<del>22 September 2021</del>	<del>26</del>	<del>136</del>	<del>19</del>	<del>1.4</del>
<del>21 October 2021</del>	<del>34</del>	<del>182</del>	<del>18</del>	<del>1.3</del>
<del>2 April 2022</del>	<del>n.m.</del>	<del>64</del>	<del>n.m.</del>	<del>n.m.</del>
<del>20 May 2022</del>	<del>n.m.</del>	<del>733</del>	<del>n.m.</del>	<del>n.m.</del>
<del>5 July 2022</del>	<del>91</del>	<del>306</del>	<del>30</del>	<del>2.1</del>
<del>13 August 2022</del>	<del>47</del>	<del>203</del>	<del>23</del>	<del>1.6</del>
<del>11 October 2022</del>	<del>27</del>	<del>140</del>	<del>19</del>	<del>1.4</del>

~~n.m.~~<sup>?)</sup>: No measurement possible

#### 4.1.2 Continuous discharge measurements at AP10 (downstream location)

The water table discharge correlation obtained for the downstream location at AP10 is shown in Fig. 3. Above a discharge of ca. 60 L s<sup>-1</sup>, the data nicely follow a polynomial correlation. Nevertheless, we consider discharge estimates below 100 L s<sup>-1</sup> as unreliable because this is exclusively the case in winter when the stream is partially and periodically covered by ice and

snow, strongly affecting the hydraulics (i.e. the relevant cross section of the stream) at the measurement location. Thus, for 2021 and 2022 continuous discharge estimates are only used for the period between May and October. The continuous discharge data are presented with the seasonal flux estimates below.

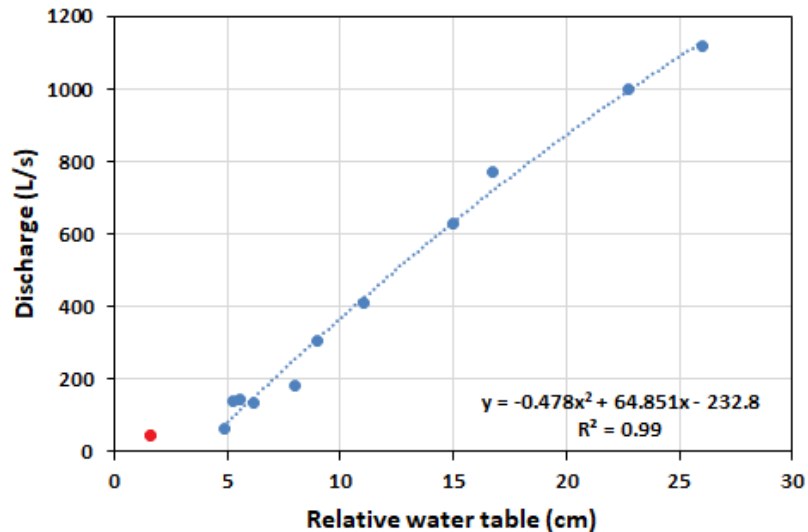


Figure 3: Correlation between water table and manual discharge measurements at the AP10 location and the derived polynomial correlation for water tables above 5 cm. At lower water tables, the correlation does not work, likely because such low values are observed in wintertime, when the hydraulics at the measurement location are strongly affected by ice. This is manifested by the measurements conducted on 23 March 2021, yielding a discharge of  $53 \text{ L s}^{-1}$  (red dot).

#### 4.2 Chemical composition of the streamwater

Table 2 presents the concentration range of selected solutes in streamwater samples collected from all five sampling locations. The full analyses are provided in the Supplement (Tables S24-S75). The temperature of the three rock glacier springs at the origin of the Aua da Prasüra stream (AP1, AP2, and AP3, Fig. 1) were constantly below  $2 \text{ }^{\circ}\text{C}$ , confirming that all springs originate from an intact rock glacier containing ice-rich permafrost as indicated by the permafrost and ground ice map shown on Figure 1b (Kenner et al., 2019) (Fig. 2). At AP1-AP3, the concentrations of Al, F<sup>-</sup>, Mn, and Ni were almost always above the corresponding drinking water limits. The highest concentrations were found at AP1, discharging at the lowest altitude (2660 m a.s.l., Figs. 1, 2). Here, the concentrations reached values up to  $28.7 \text{ mg L}^{-1}$  Al,  $23.1 \text{ mg L}^{-1}$  F<sup>-</sup>,  $11.3 \text{ mg L}^{-1}$  Mn, and  $3.3 \text{ mg L}^{-1}$  Ni. In the cases of Mn and Ni, these correspond to a very strong exceedance of the Swiss drinking water limit by factors of 226 and 165, respectively. For Al and F<sup>-</sup>, the situation is less severe, but the drinking water limits were still exceeded by factors of up to 143 and 15, respectively. At the other two rock glacier springs (AP2, AP3), the

330 concentrations were lower and decreased with increasing altitude (Table 2). For instance, the maximum concentration of Ni at AP2 (2700 m a.s.l.) and AP3 (2770 m a.s.l.) were 1.6 and 0.4 mg L<sup>-1</sup>, respectively, and thus 2 and 8 times lower than at AP1. In contrast to the other solutes of interest, the Swiss drinking water limit for Zn (5 mg L<sup>-1</sup>) was only periodically exceeded at the lowest rock glacier spring (AP1).

335 Downstream of the rock glacier springs, the temperature and pH gradually increased, while the solute concentrations decreased as manifested by the streamwater samples collected at [AP1 2](#), AP5 and AP10 (Table 2). Nevertheless, 5 km downstream and at an altitude of 1890 m a.s.l., the concentrations of Mn ( $\leq 0.37$  mg L<sup>-1</sup>) and Ni ( $\leq 0.24$  mg L<sup>-1</sup>) at AP10 (Fig. 1) still exceeded the drinking water limits by factors of up to 7 or 12, respectively.

340 **Table 2: Chemical composition of streamwater samples from different locations along the Aua da Prasiira stream (Fig. 1)**

Location	Number of samples	Altitude (m a.s.l.)	T (°C)	pH	EC ( $\mu\text{s cm}^{-1}$ )	TDS (mg L <sup>-1</sup> )	Al (mg L <sup>-1</sup> )	Mn (mg L <sup>-1</sup> )	Ni (mg L <sup>-1</sup> )	Zn (mg L <sup>-1</sup> )	As ( $\mu\text{g L}^{-1}$ )	F (mg L <sup>-1</sup> )	SO <sub>4</sub> (mg L <sup>-1</sup> )
AP1	5	2660	0.8-1.4	4.7-5.0	1197-2040	1819-3942	<b>15.4-28.7</b>	<b>4.8-11.3</b>	<b>1.70-3.30</b>	<b>4.20-7.81</b>	<4-4.1	<b>2.1-23.1</b>	1354-2803
AP2	5	2700	0.3-3.1	5.1-5.2	160-711	559-3083	<b>2.7-10.9</b>	<b>0.3-3.4</b>	<b>0.35-1.63</b>	0.74-2.49	<4	<b>0.4-5.6</b>	415-1986
AP3	6	2770	0.7-4.7	5.8-6.4	403-1625	519-1616	<b>0.5-1.5</b>	<b>0.009-0.191</b>	<b>0.05-0.39</b>	0.12-1.16	<4	<b>1.4-4.3</b>	369-1008
<a href="#">AP1 2</a>	<b>6</b>	<b>2545</b>	<b>2.1-7.6</b>	<b>4.8-5.3</b>	<b>1199-1527</b>	<b>1470-2458</b>	<b>9.4-13.7</b>	<b>1.9-3.2</b>	<b>1.2-1.8</b>	<b>2.8-4.2</b>	<b>0.8-11</b>	<b>0.5-11.9</b>	<b>1083-1821</b>
AP5	8	2530	1.4-8.9	5.3-5.7	317-1208	388-1689	<b>1.4-8.3</b>	<b>0.079-1.729</b>	<b>0.18-1.22</b>	0.56-3.01	<4	<b>0.5-6.5</b>	285-1287
AP10	39	1890	0.6-11.4	6.0-8.1	133-440	117-507	<b>0.01-0.41</b>	<b>0.007-0.365</b>	<b>0.02-0.24</b>	0.05-0.62	<4	<b>0.5-1.8</b>	80-327
<sup>1</sup> Drinking water limit							0.2	0.05	0.02	5	0.01	1.5	

<sup>1</sup><https://www.fedlex.admin.ch/eli/cc/2017/153/de>

Cells in bold indicate concentrations above drinking water limit

#### 4.2.1 Seasonal variation of concentrations of toxic soluteelements

At the downstream monitoring location AP10 (Fig. 1), the concentrations of Ni, Zn and F<sup>-</sup> showed strong linear correlations with the electrical conductivity measured by the installed probe as evidenced by linear correlation coefficients (R<sup>2</sup>) of at least 0.91 (Fig. 3). The correlations are caused by constant ratios between these concentrations and the concentration of sulfate (Figure S4, Supplement), displaying by far the highest values of all solutes in our streamwater samples and hence controlling the measured EC (Table 2, S2-S7, Supplement). Accordingly, the conductivity data recorded by the probe allow to continuously estimating the concentrations of these three solutes using the derived linear calibration curves. For Mn and other reactive solutes such as Al, the correlation between concentrations and conductivity values is poor (Fig. 3), which means that these concentrations cannot be estimated using the conductivity data.



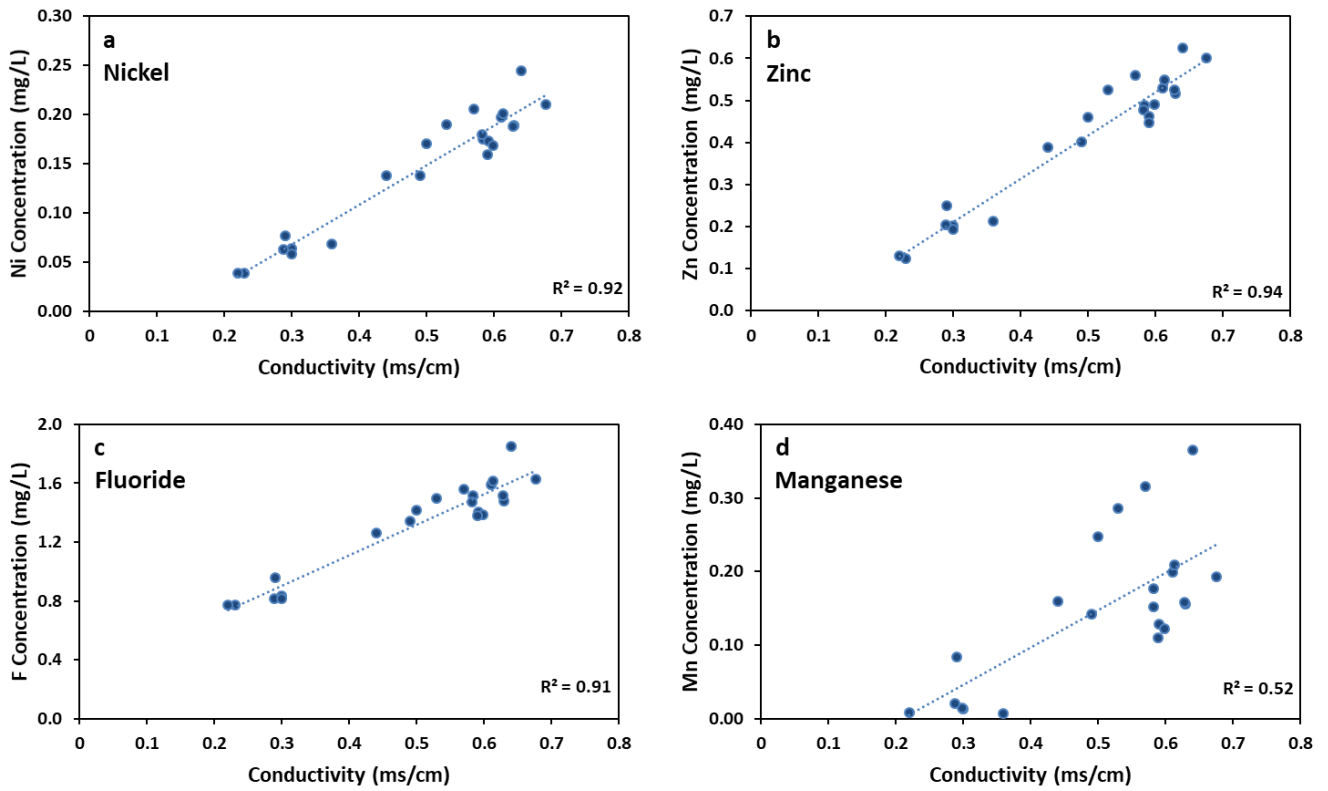
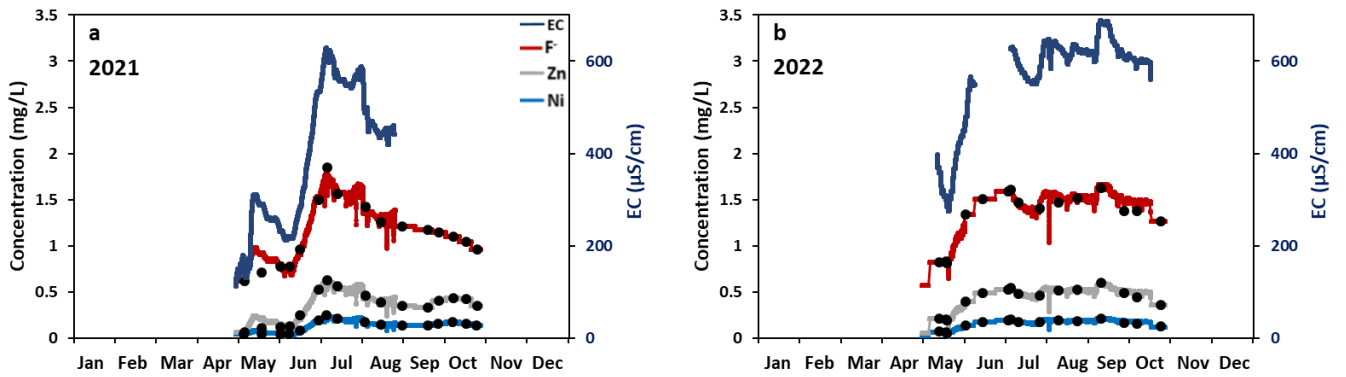


Figure 3: Linear correlations at the downstream monitoring location AP10 between electric conductivity (EC) measured by the installed probe and concentrations of selected solutes. (a) Ni. (b) Zn. (c) F. (d) Mn. Merged data from 2021 and 2022.

355



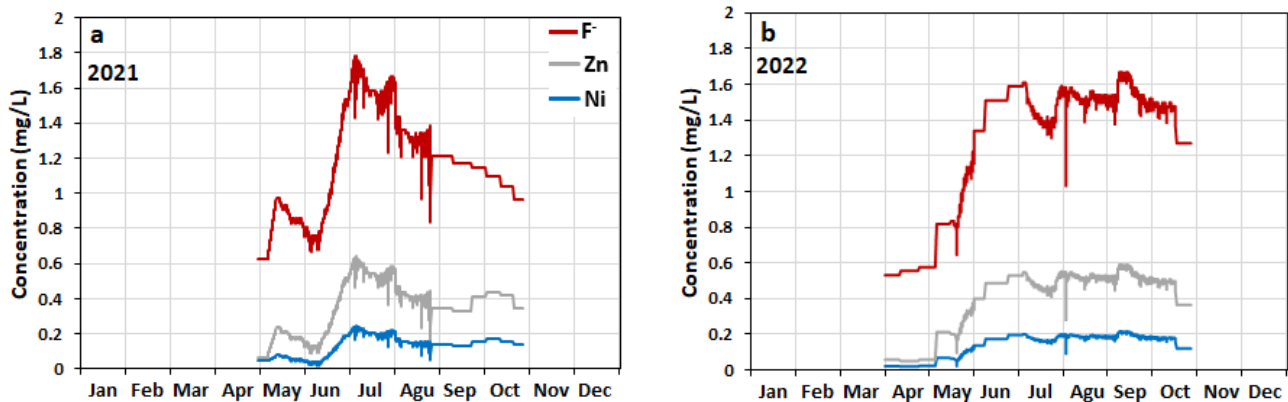
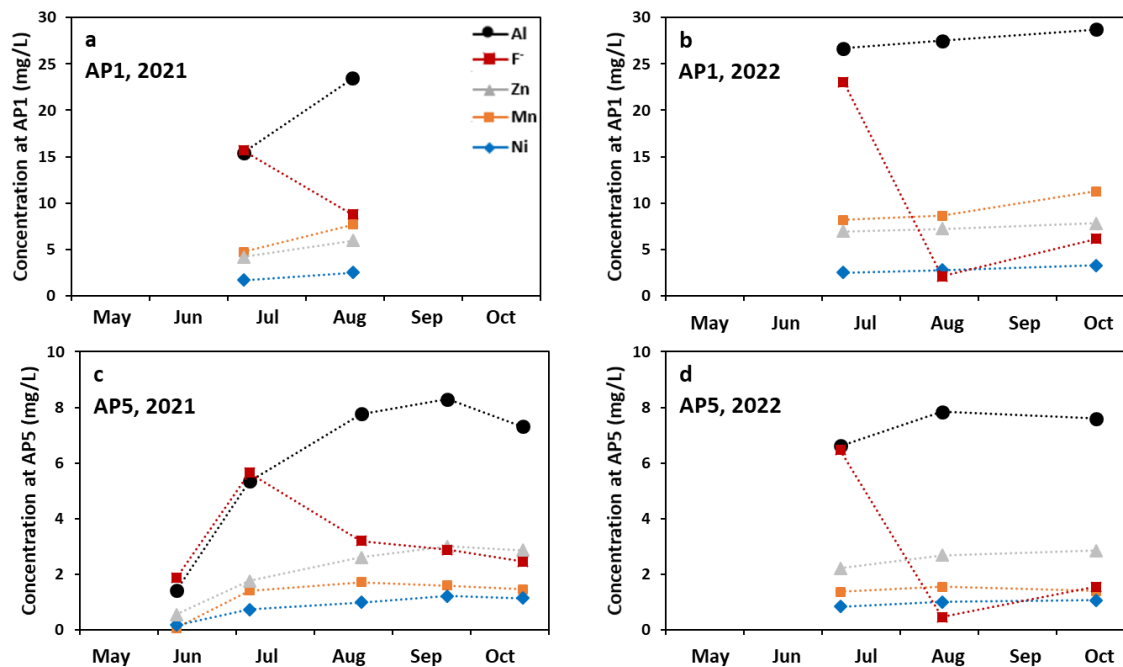


Figure 4: Seasonal evolution of the EC (right-hand y-axis) and the concentrations of F<sup>-</sup>, Zn, and Ni (left-hand y-axis) at the downstream monitoring location, API0, estimated based on the electrical conductivity data and the correlations shown in Figure 3. (a) 2021, (b) 2022. The black filled circles on each curve show the actual solute concentrations measured on the bi-weekly collected water samples (Table S2, Supplement). As, the EC data was not reliable for the following periods: 1 May to 14 May 2021, 29 August to 30 October 2021, 1 May to 20 May 2022, 7 Jun to 7 Jul 2022, and 21 October to 30 October 2022, a linear interpolation of the chemical analysis of the biweekly samples was employed for the mentioned periods to estimate the seasonal evolution of the solute concentrations. Because of the unreliability of EC data, a linear interpolation of the chemical analysis of the biweekly samples (Table S1, Supplement) was employed for the following periods: 1–14. May 2021, 29. Aug–30. Oct 2021, 1–20. May 2022, 7. Jun–7. Jul 2022, and 21–30. Oct 2022.

Figure 4 illustrates the seasonal variations of the EC and the concentrations of F<sup>-</sup>, Zn, and Ni estimated for the downstream monitoring location API0 based on the conductivity data and the correlations shown in Fig. 3. The black-filled circles on each curve represent the actual solute concentrations measured on the bi-weekly collected water samples, demonstrating that the continuously estimated concentrations are reliable. For both monitoring years, these solutes showed maximum concentrations in summer, although the seasonal behavior was slightly different in the two years. In 2021, the highest concentrations were estimated for early July followed by a gradual decrease until the end of the monitoring period at the end of October, except for short-term excursions where the concentrations periodically increased. In 2022, with the exception of short negative and positive excursions, the concentrations were nearly constant from early July to mid-September. For both monitoring years, the concentrations at the end of the monitoring period were roughly twice as high as at the beginning of the monitoring period in May. In contrast to the downstream monitoring location API0, at the upstream monitoring location AP5 as well as at the most frequently sampled rock glacier spring API1, the concentrations of the solutes except F<sup>-</sup> (i.e. Al, Ni, Zn and Mn) generally increased during the May-October monitoring period and the highest values were measured towards the end of the monitoring period (Fig. 5).



385

Figure 5: Seasonal variation of the concentrations of Al, F<sup>-</sup>, Zn, Mn, and Ni at the rock glacier spring AP1 and the upstream discharge monitoring location AP5 (Fig. 1). (a), (b) Interpolation of solute concentrations of samples taken at AP1 in 2021 and 2022, respectively. (c), (d) Interpolation of solute concentrations of samples taken at AP5 in 2021 and 2022, respectively.

### 390 4.3 Seasonal evolution of mobilized fluxes

#### 4.3.1 Manual flux measurements (AP1 2, AP5 and AP10)

At the ~~two-three discharge~~ monitoring locations AP1 2, AP5 and AP10 (Fig. 1), we took 6, 8 and 10 flux measurements, respectively. Figure 6 presents the fluxes of Al, F<sup>-</sup>, Zn, Mn, and Ni. All fluxes showed a very similar pattern with a strong seasonal variation. In both years, the highest fluxes occurred in early July except for AP10, where in 2022 the maximum flux of F<sup>-</sup> was observed in May. Among the five solutes, Al and F<sup>-</sup> displayed the highest fluxes with values exceeding 100 kg per day at AP5 in July 2021. On the same sampling day, the fluxes of Zn, Mn, and Ni reached maximum values of 20-40 kg per day. In early and late summer, the fluxes were up to one order of magnitude lower.

At specific sampling dates, the ~~two-three~~ monitoring locations exhibited ~~very~~-similar fluxes for Zn and Ni (Fig. 6, Table S1, Supplement). In contrast, the fluxes of Mn and Al were significantly lower at the downstream location (AP10), while in fall the flux of F<sup>-</sup> was slightly higher at AP10 than at AP5. ~~is slightly higher in fall when the discharge is low.~~ These

400

observations suggest that at AP10, only the fluxes of Zn and Ni may serve as a proxy for the processes occurring in the rock glacier at the source of the stream (see Discussion below).

405

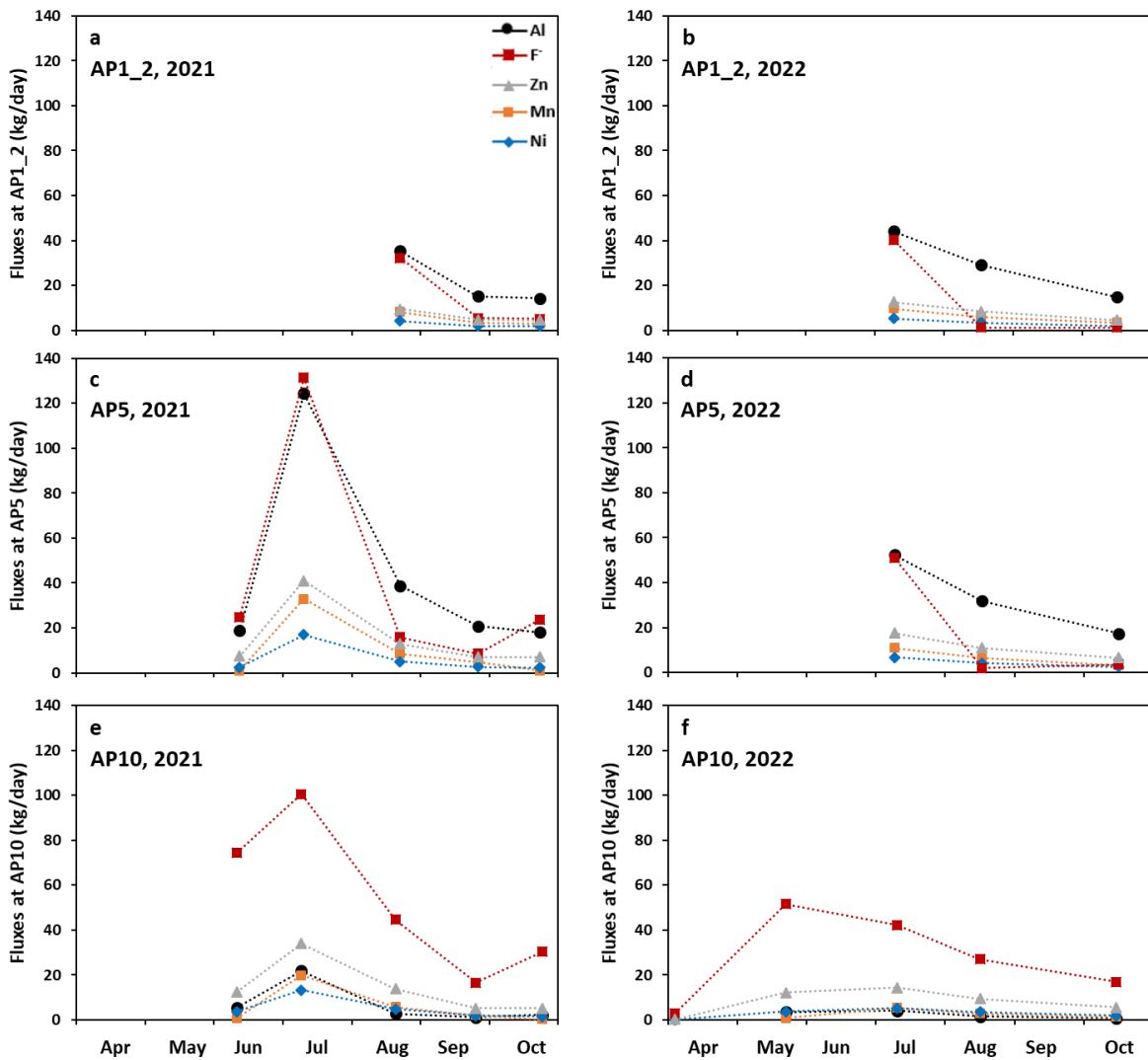


Figure 6: Extrapolated ~~F~~ fluxes of Al, F, Zn, Mn, and Ni at the three ~~two~~ main monitoring stations along the Aua da Prasiura stream. (a), (b): Fluxes measured at the AP1\_2 location in 2021 and 2022. (c), (d): Fluxes measured at the upstream AP5 location in 2021 and 2022. (e), (f): Fluxes measured at the downstream AP10 location in 2021 and 2022 ~~at the downstream AP10 location~~.

#### 410 4.3.2 Automatic flux estimation (AP10)

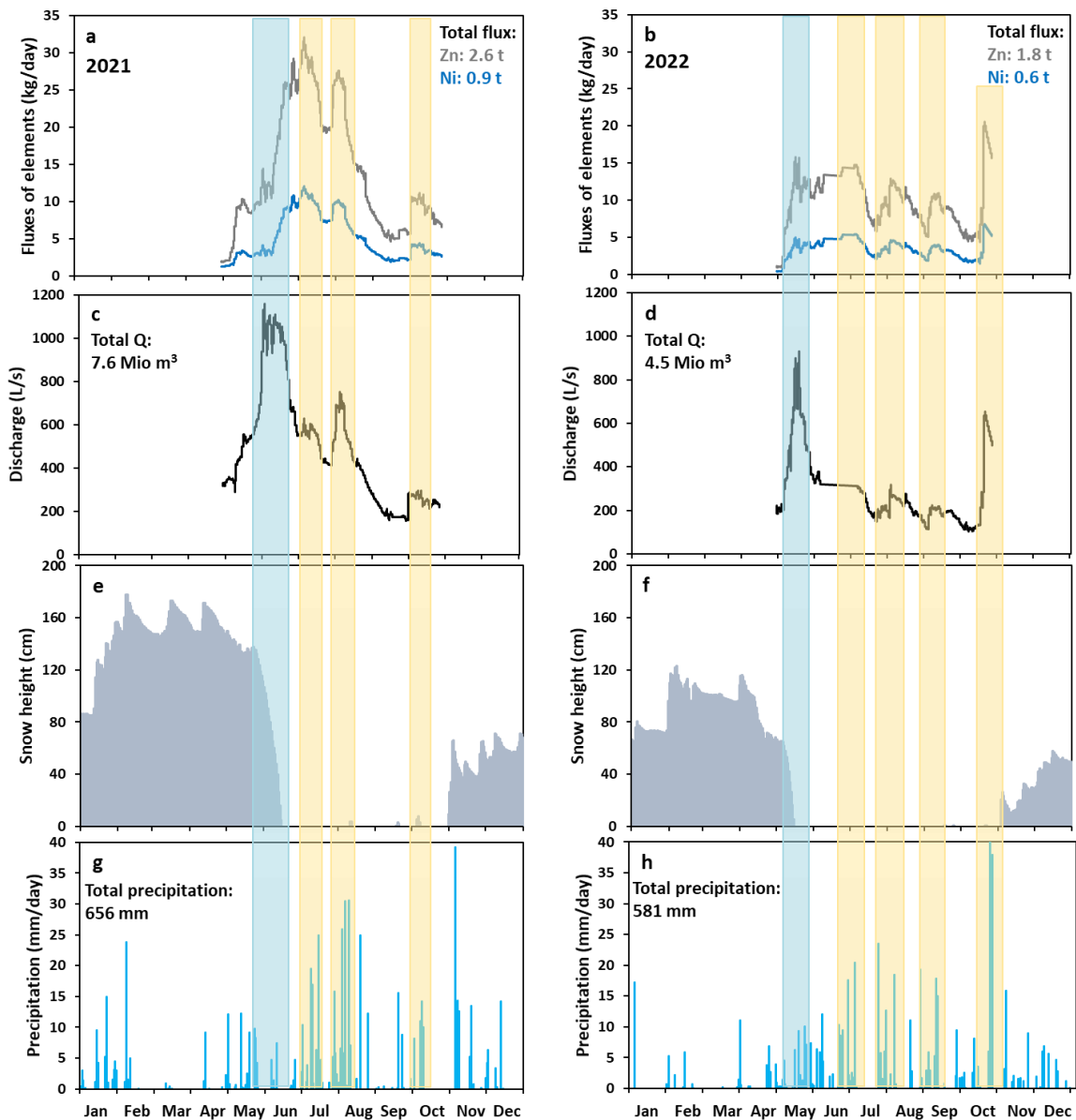
The fluxes of Zn and Ni continuously estimated at the downstream monitoring location AP10 are shown in Fig. 7. Integrating the fluxes for the 2021 monitoring period yielded surprisingly high total fluxes of 2570 and 940 kg for Zn and Ni, respectively. For the same period in 2022, the total fluxes for these two solutes were 1830 and 650 kg, respectively, and hence 29-31 % lower than in 2021.

415

The seasonality of the estimated Ni and Zn fluxes was rather similar. In both monitoring years, the lowest values were observed at the beginning of the monitoring period in early May when the rock glacier at the origin of the stream was still covered by snow. During snowmelt, the increase in discharge was immediately followed by a rapid surge of the two fluxes, demonstrating a very strong correlation between discharge and solute fluxes. Consequently, synchronous discharge and flux peaks are observed during peak snowmelt conditions (Fig. 7a, b). In 2021, this was the case in mid-June. In 2022, the winter snow cover was less (Fig. 7c), peak snowmelt conditions occurred about 3 weeks earlier at the end of May, and the corresponding discharge and ~~soluteelement~~ fluxes were significantly lower than in 2021. After the snowmelt peaks, additional synchronous flux and discharge peaks occurred during heavy rainfall events. In 2021, this was the case in early July, early August, and early October (Fig. 7d). In 2022, such short-term discharge and flux peaks occurred in response to ~~precipitation-rainfall~~ events in early July, early August, mid-September and mid-October. In addition to the simultaneously occurring flux and discharge peaks (Fig. 7a, b), the strong correlation between the two parameters was also manifested by very similar patterns of their seasonal behavior in both monitoring years (Fig. [S5](#)).

420

425



430

Figure 7: Seasonal evolution of key parameters recorded through the two monitoring years. (a), (b): Fluxes of Zn and Ni **estimated calculated for at** the downstream monitoring location AP10 (**compare** Fig. 1) in 2021 and 2022, respectively. (c), (d): Discharge of the Aua da Prasüra stream measured at the same location (**AP10**) in 2021 and 2022, respectively. (e), (f): Snow height recorded in 2021 and 2022 at the Murtaröl snow station, **located some 15 km Northwest of AP10 at an altitude of 2359 m a.s.l.** (SLF, 2023). (g), (h): Rainfall recorded in 2021 and 2022 at the Santa Maria weather station, **located some 6.5 km North of AP10 at an altitude of 1388 m a.s.l.** (MeteoSwiss, 2023). The light blue bars highlight synchronous discharge and flux peaks observed during snowmelt peak in June 2021 and May 2022. The yellow bars mark synchronous peaks in discharge and **solute element** fluxes after

435

~~precipitation-rainfall~~ events. Due to technical problems, no reliable discharge data were obtained in June 2022. Therefore, a linear interpolation was used to retrieve the data from 7 June to 7 July. Technical problems also occurred from 24 October to 31 October 2022 in response to a heavy rainfall event. For this event, a recession curve with  $Q_0 = 668 \text{ L s}^{-1}$  and  $a = 0.00235$  (Eq. (1), Supplement) was applied to correct for the missing discharge data.

## 5 Discussion

### 5.1 Tracking of toxic ~~soluteelement~~ fluxes exported from the studied rock glacier

The observation that the fluxes recorded at AP5 and AP1\_2 yielded similar values (Fig. 6; Table S1, Supplement) implies that the majority of the fluxes measured at AP5 originate from the rock glacier shown on Figure 2. In case of Ni, 75-88 % of the fluxes at AP5 are already recorded at AP1\_2, while for Zn, the contribution from AP1\_2 at AP5 ranges between 64 and 77 % (Table S1, Supplement). The difference to 100% is explained by subsurface flow not captured at AP1\_2, minor contributions from other ice-rich permafrost features (Fig. 2), and contributions from AP3. The comparison of the Ni and Zn fluxes recorded at AP5 and AP1\_2 thus confirms the earlier finding of Wanner et al. (2023) that ice-rich permafrost in general and intact rock glaciers in particular operate as strong and long-lasting chemical reactors causing high concentrations of toxic solutes in the corresponding rock glacier springs.

#### 5.1.1. Conservatively behaving solutes (Ni, Zn)

In the studied system, the strong chemical signal in the rock glacier springs AP1 and AP2 (Table 1) allows us to continuously track the concentrations and fluxes of conservatively behaving toxic solutes at the well-accessible downstream monitoring location AP10 (Fig. 1) using a conductivity probe. This probe is installed at a well accessible site, located ca. 5 km downstream of the rock glacier at an altitude, which is about 800 m lower than the lowest rock glacier spring. This mainly applies to Ni and Zn as manifested by the observation that at specific sampling dates, these solutes exhibit similar fluxes at the upstream (AP5) and downstream (AP10) monitoring locations (Fig. 6; Table S1, Supplement). In general, they were about 5-20 % lower at AP10 except for low flow conditions, when they were up to 35% lower but not strongly affecting annual fluxes (e.g., September and October 2021 and 2022). Moreover, the quasi-conservative behavior of Zn and Ni along the stream is confirmed by their constant concentration ratios at the two monitoring locations (Fig. S4a, b, Supplement). This implies that the mobilization of Ni and Zn is not strongly retarded by basaluminite precipitated along the stream, although Ni enrichment in basaluminite has been previously documented (Thies et al., 2017; Wanner et al., 2023). Likewise, this indicates that downstream of AP5, there are no significant additional sources for these solutes. Thus, the fluxes of Ni and Zn monitored at AP10 exclusively originate from ice-rich permafrost upstream of AP5, whereby the majority (up to 88%) is exported from the studied rock glacier.

470 Despite their conservative behavior, the seasonal concentration patterns for Zn and Ni vary along the stream (Figs. 4, 5). Near the rock glacier source, concentrations of Ni and Zn (and other solutes) display an increasing trend throughout the summer (AP1, AP5, Fig. 6). In contrast, concentrations peaks are observed in early summer at the downstream location (AP10, Fig. 5). This contrasting behavior is due to the fact that all concentrations are controlled by the amount of solutes being mobilized from the rock glacier and the degree of dilution by snowmelt and rainwater. Due to the strong difference in the catchment sizes at these three sampling locations (AP1: 0.04 km<sup>2</sup>, AP5: 1.33 km<sup>2</sup>, AP10: 9.41 km<sup>2</sup>), the degree of dilution is strongly different, causing the observed variation of the concentration patterns along the stream. Because of the strong impact of dilution, we propose that tracking solute fluxes is more useful than solute concentrations to quantitatively understand the seasonality of the mobilization of toxic solutes from the rock glacier. Solute fluxes correspond to the product between solute concentrations and the discharge and hence account for dilution effects by snowmelt and rainwater, which both show strong seasonal variations.

### 480 **5.1.2. Other solutes (Al, Mn, F<sup>-</sup>)**

In contrast to Ni and Zn, at the downstream monitoring location AP10 (Fig. 1), the fluxes of solutes that do not behave conservatively or of those affected by additional sources, do not reflect mobilization from ice-rich permafrost upstream of AP5. In case of Al, this is because most of it precipitates as basaluminite along the stream as manifested by the white-colored bedload downstream of AP5 (Fig S1, Supplement). Manganese behaves reactive because the oxidizing conditions in the stream lead to a continuous oxidation and precipitation of Mn, originally mobilized by the reduction of Mn oxides in the rock glacier at the origin of the stream (Wanner et al., 2023). Thus, the concentration of Mn at the downstream location AP10 is not only controlled by the mobilization in the rock glacier but also by the degree of oxidation along the stream, which is a slow, kinetically-limited process (Diem and Stumm, 1984). The amount of Mn lost due to oxidation along the stream strongly depends on the seasonally variable residence time of streamwater in the monitored catchment, which is the reason why the correlation between concentration and conductivity is poor (Fig. 3). The flux of F<sup>-</sup> (Fig. 7) varies downstream of AP5 because the tributaries merging with the main Aua da Prasūra stream may also contribute to the F<sup>-</sup> flux measured at AP10. This is particularly relevant at low flux conditions in spring and fall, when the fluxes of F<sup>-</sup> are usually higher at AP10 than at AP5 (Fig. 6).

495 Because of their reactive behavior, the total fluxes of Al, F<sup>-</sup>, and Mn exported from the rock glacier in each monitoring period can only be estimated based on a combination of several data. In particular, these are sporadic manual flux measurements carried out near the rock glacier outlet at AP5, their comparison with the fluxes of Zn and Ni, which are not affected by any chemical reactions occurring along the stream (Fig. 6), and the total fluxes for Zn and Ni estimated at AP10 (Fig. 7a). For Al and F<sup>-</sup>, this yields annual fluxes of about three times higher than those estimated for Zn (i.e. up to 10 t and 7 t in 2021 and 2022, respectively). For Mn, the annual fluxes exported from the rock glacier were between those of Ni and Zn (2021: 940-2570 kg; 2022: 650-1830 kg). Therefore, to quantitatively understand the seasonality of the mobilization of toxic



~~elements from the rock glacier, we propose that tracking the mobilized fluxes is more useful than element concentrations. This is because element fluxes correspond to the product between element concentrations and the discharge and hence account for dilution effects by snowmelt and rainwater, which both show strong seasonal variations. The continuous monitoring of rock glacier springs is challenged by their remote location at high altitude and rugged topography.~~

## **5.2 Controls on soluteelement mobilization from intact rock glaciers ~~:- insights on ice melt export rates~~**

The very strong correlation between the flux and discharge curves implies that the amount of water infiltrating into the rock glacier system plays a crucial role in controlling the export of solutes from the rock glacier at the origin of the studied stream. This is not only manifested by the simultaneously occurring discharge and flux peaks (Fig. 7a,b) as well as the very similar behavior of the flux and discharge curves (Fig. S5); but also by the difference in the total discharge calculated for the two monitoring years and in the annual fluxes of toxic solutes.- In 2022, when the total fluxes of Zn and Ni ~~and consequently the export of ice melt~~ from the rock glacier were about 30 % lower than in 2021, the total discharge between May and October was 41 % lower than in 2021 (Figs. ~~7b7c, d~~). The lower discharge in 2022 resulted from the lower winter snow cover and the lower amount of precipitation in summer (Figs. ~~7e-h~~).

Owing to the kinetic limitation of the oxidation rate of pyrite and other sulfuric acid generating sulfides (Williamson and Rimstidt, 1994), the very quick increase of solute fluxes observed after hydraulic events (Fig. 7) confirms our hypothesis that processes in addition to chemical weathering (i.e. ARD) are responsible for the high concentrations and fluxes of toxic solutes observed today in the studied catchment (Wanner et al., 2023). Figure 8 presents conceptual models consistent with current thermal, hydraulic and chemical observations of intact rock glaciers to explain the causes for the highly prominent role of water infiltration on controlling the export of toxic solutes from intact rock glaciers. In particular, the models show that the recorded mobilization of toxic solutes reflects the last step of a complicate sequence of coupled processes including (i) the oxidation of sulfide producing sulfuric acid and promoting the dissolution of solutes from the host rock (i.e. ARD), (ii) temporal storage and long-term enrichment of the dissolved solutes in rock glacier ice, and (iii) their final hydraulic mobilization during climate-change induced accelerated degradation of rock glaciers. The individual steps are described below.

### **5.2.1. Weathering by sulfuric acid and storage of dissolved solutes in rock glacier ice (Steps (i) and (ii), Fig. 8a)**

The current understanding of rock glacier hydrology is that the movement of subsurface water follows two distinct flow paths. In Figure 8, these are referred to as "quick flow" and "base flow," which occur within the seasonally frozen active layer and the permanently unfrozen base layer, respectively (Giardino et al., 1992; Krainer and Mostler, 2002; Jones et al., 2019). Additionally, subsurface flow through the frozen core (i.e. the sediment-ice mixture), known as intra-flow or slow

535 internal flow, was discovered through dye-tracing experiments (Tenthorey, 1992). Furthermore, as reported for the Lazaun  
rock glacier, temperatures at or even above 0 °C are observed towards the top of the frozen rock glacier core in late summer,  
i.e. in August and September (Krainer et al., 2015; Nickus et al., 2023), indicating the presence of liquid water promoting  
intra-permafrost flow. Such fluid flow has been mainly documented in the frontal sections of active rock glaciers, which has  
significant implications on rates of creep and stability of rock glaciers (Jones et al., 2019; and references therein). In turn, the  
540 deformation of rock glacier cores leads to the formation of networks of air voids and fractures, providing positive feedback  
on intra-permafrost fluid flow.

The presence of liquid water in rock glaciers is a prerequisite for the chemical interaction with the rock glacier sediments  
(Wanner et al., 2023). Moreover, it introduces oxygen into the system, promoting the oxidation of sulfides (e.g., pyrite) and  
545 thus the generation of sulfuric acid as main weathering agent. Based on its fine-grained nature and high reactive surface  
areas, the water-saturated base layer is the obvious candidate for the production of sulfuric acid and strong toxic solutes  
mobilization. Despite a groundwater residence time of several months in the base layer (Jones et al., 2019), however, this is  
inconsistent with recent experiments showing that the interaction between fine-grained pyrite-bearing paragneiss of the  
Eastern Alps does not reproduce the high concentrations of toxic solutes in streams discharging from intact rock glaciers  
550 (Wanner et al., 2023). Accordingly, toxic solute mobilization must be dominated in other parts of the rock glacier system.  
Since the active layer mainly consist of large rocks with very low reactive surface area, the fine-grained sediment-ice  
mixture in the rock glacier core is the only other plausible alternative.

In the rock glacier core, liquid water mainly occurs in late summer and towards the top. If the amount of liquid water is  
555 limited and no fully connected water film can develop (Fig. 8a), toxic solutes mobilized from the sediments remain within  
the rock glacier and their concentrations in the rock glacier spring are low. Owing to recurring cycles of freezing and  
thawing within the sediment-ice mixture, however, with time this leads to a continuous enrichment and interim storage of the  
leached solutes in the rock glacier ice. We hypothesize that this scenario is at play at high altitude or under colder climatic  
conditions than today, where the amount of ice in the rock glacier is stable. However, more research is required on how  
560 much time for the enrichment of toxic solutes in the rock glacier ice is needed to cause the high solute concentrations  
currently observed in the studied rock glacier springs. If the climatic conditions are too cold for seasonal temperatures at or  
above 0 °C, the rock glacier core is chemically inert, and the accumulation of solutes pauses.

### **5.2.2 Climate change accelerated mobilization of toxic solutes (Step (iii), Fig. 8b)**

565 In the recent years, climate warming likely led to an increase of the time when the temperature at the top of the frozen core  
of the studied rock glacier is at or above zero. The same applies to the corresponding maximum temperature in summer.  
Consequently, the amount of liquid water (i.e. ice melt) increases, and a fully connected water film enriched in toxic solutes

570 may develop towards the top of the rock glacier core (i.e. at the top of the sediment-ice mixture) in late summer (Fig. 8b). During this time of the year, this leads to a gravity-driven, vertical export of ice melt enriched with toxic solutes to the base layer. During heavy rainfall events intra-permafrost flow becomes highly significant and the export to the base layer and also to the rock glacier springs is strongly accelerated. In late summer, this is the main reason for the simultaneously occurring flux and discharge peaks (Fig. 7). Since rock glaciers represent high-altitude aquifers with a high water storage capacity and groundwater residence time on the order of several months (Jones et al., 2019; Wagner et al., 2020, 2021a, b), however, some of the toxic solutes exported from the rock glacier core are not immediately transported to the rock glacier springs and

575 remain in the unfrozen base layer aquifer during wintertime. Stagnant water bodies enriched in toxic solutes may be present also elsewhere in the rock glacier system (i.e., outside the base layer). With the infiltration of snowmelt in the following summer, the water table raises and the hydraulic head gradient in rock glacier aquifer increases (Fig. 8b). This quickly accelerates the discharge of groundwater and stagnant water enriched in toxic solutes and causes the simultaneously occurring flux and discharge peaks observed during snowmelt (Fig. 7). Such hydraulic mobilization of toxic solutes

580 previously exported from the rock glacier core to the base layer is consistent with the fact that during snowmelt the 0 °C isotherm is near the surface (Williams et al., 2006) and that no export of ice melt enriched in toxic solutes to the base later can happen at this time of the year.

585 In late summer, when the 0 °C isotherm is below the top of the rock glacier core, the infiltration of rainwater into the system brings thermal energy to the rock glacier core (Rist and Phillips, 2005; Williams et al., 2006), further promoting the degradation of the sediment-ice matrix in addition to the hydraulic effect described above. This is particularly relevant under increased intra-permafrost flow, where the contact area between the ice and water is elevated.

590 For the studied rock glacier in Val Costainas, the coupled thermal-hydraulic-chemical processes discussed above and shown on Figure 8 are likely very active. This results in an accelerated degradation of the rock glacier ice accompanied by a strong mobilization of toxic solutes. In particular, this is manifested by the disproportionately high discharge from the rock glacier (Table 1) and the remarkable export rates of toxic solutes, which are on the order of several tons per year (Fig. 7).~~the degradation of the rock glacier ice is significant enough to cause a disproportionately high discharge at the monitoring site AP5, located a few hundred meters downstream of the rock glacier (Table 1). Given that there are other rock glaciers in the~~

595 Val Costainas catchment (Fig. 1a) and that the catchment is widely covered with other quaternary landforms such as talus, moraines, and alluvial cones characterized by significant water storage capacities (Arnoux et al., 2020, 2021), the strongly elevated discharge contribution at AP5 is quite remarkable. While it confirms the general potential of rock glaciers for subsurface water storage (Wagner et al., 2020; 2021b), it demonstrates that the rock glacier at the origin of Aua da Prasūra is currently very active hydraulically.

600

605 Since the frozen rock glacier core is likely heavily enriched with toxic elements, the coupled thermal hydraulic degradation of the rock glacier ice is manifested by high concentrations in the lowest rock glacier spring AP1 (Fig. 5). In contrast, under dry conditions, the frozen rock glacier core is insulated from the hot summer temperatures at the surface (Hanson and Hoelzle, 2004; Humlum, 1997) and stagnant water films are protected from water driven export and their export is limited by gravity. Consequently, the export of both ice melt and toxic elements remains rather low under dry conditions as observed in 2022 (Figs. 7, 8). Additionally, the lowest concentrations are observed in the AP3 spring discharging at the highest elevation (2770 m a.s.l. Table 2). Here, the temperature is still too low to generate a continuous water film in late summer and the export of ice melt and toxic element concentrations are low. With decreasing elevation, export of ice melt, and hence, the concentrations of toxic elements strongly increase while the discharge may be significantly affected by ice melt.

610 At the AP1 spring, located at an altitude of 2660 m a.s.l. (Figs. 1, 2) toxic element concentrations reach maximum values exceeding drinking water limits by factors of up to 226 (Table 2). These variations of toxic element concentrations in the different rock glacier springs sampled in this study show distinctly different modes for element enrichment and their subsequent mobilization.

615 Here, we The apparently lower ice melt export rate in 2022 is remarkable given that 2022 corresponds to a year with record high temperature in the Alps (Noetzi, J. and Pellet, 2023), as manifested by much higher summer temperature than in 2021 (Fig. S5). Accordingly, in our study area the variable infiltration of water into rock glaciers caused by a varying winter snow cover and variations in summer precipitation apparently has a much stronger effect on yearly ice melt export rates than the variation of the summer air temperature. (Williamson and Rimstidt, 1994)(Wanner et al., 2023)a of element enrichment modes (Fig. 8)in complex.

620 Owing to the kinetic limitation of the oxidation rate of pyrite and other sulfuric acid generating sulfides (Williamson and Rimstidt, 1994), the almost immediate increase of solute fluxes observed after hydraulic events (Fig. 7) confirms our hypothesis that processes in addition to chemical weathering (i.e. ARD) are responsible for the high concentration and fluxes of toxic solutes observed today in the studied catchment (Wanner et al., 2023). However, it should be noted that other

625 studies have proposed that high concentrations of solutes in rock glacier springs are at least partly due to atmospheric deposition caused by industrial activities or volcanic degassing in addition to ARD (Nickus et al., 2023; Del Siro et al., 2023). Based on the very high solute fluxes currently exported from the studied rock glaciers, only covering some 40000 m<sup>2</sup> (up to 10 t/a for trace elements like Al and F, see above), we consider such atmospheric sources not very likely for the studied system. This is consistent with other studies concluding that atmospheric deposition could be excluded as a main

630 cause for high solute concentrations in rock glacier springs (Thies et al., 2007; Steingruber et al., 2021). Moreover, a systematic monitoring of more than 150 rock glacier springs in Austria (Wagner et al., 2019) indicates that the enrichment of elements like Ni, Zn, Mn, Al, and sulfate occurs primarily in pragneissic geological settings but not in rock glacier draining other lithologies, which would likely be the case if atmospheric sources were relevant.

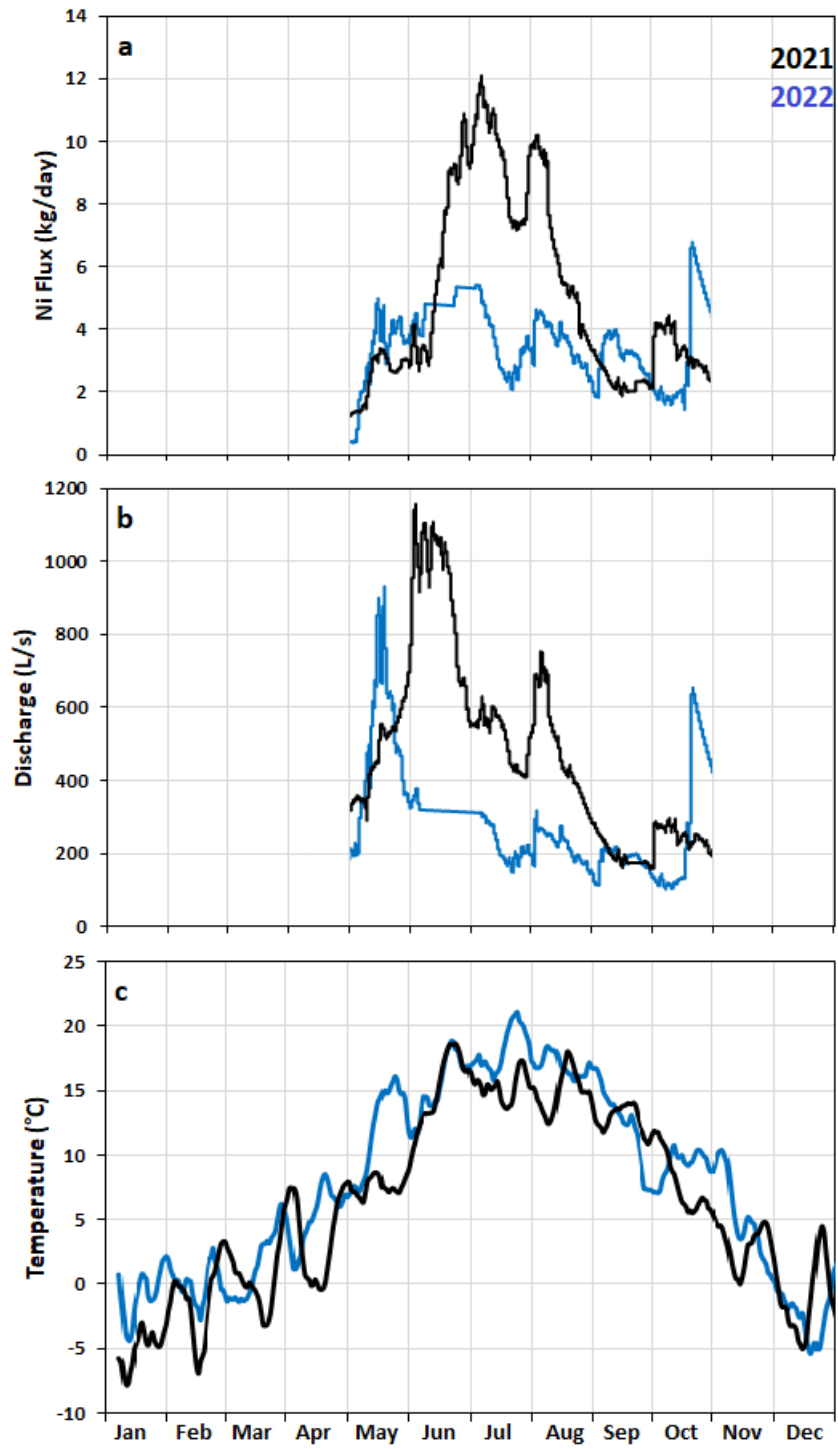


**Figure 9: Comparison of selected parameters between the two monitoring years. (a) Ni fluxes estimated at AP10; (b) Discharge at AP10. (c) Daily average temperature at the MeteoSwiss weather station at St. Maria (MeteoSwiss, 2023).**

640 The reasons for the highly prominent role of water infiltration on controlling the export of both toxic solutes and ice melt is  
illustrate by the conceptual models for element enrichment and their subsequent mobilization shown on Fig. 8. The current  
understanding of rock glacier hydrology is that the movement of subsurface water follows two distinct flow paths. In Fig. 10,  
these are referred to as "quick flow" and "base flow," which occur within the active layer (AL) and the base layer (BL),  
respectively (Giardino et al., 1992; Krainer and Mostler, 2002; Jones et al., 2019). Additionally, subsurface flow through the  
645 frozen core (i.e. the sediment ice mixture), known as intra flow or slow internal flow, was discovered through dye tracing  
experiments (Tenthorey, 1992). Furthermore, as reported for the Lazaun rock glacier, temperatures at or even above 0 °C can  
be observed towards the top of the frozen rock glacier core (Krainer et al., 2015; Nickus et al., 2023), indicating the presence  
of liquid water promoting intra permafrost flow. Such fluid flow has been mainly documented in the frontal sections of  
active rock glaciers, which has significant implications on rates of creep and stability of rock glaciers (Jones et al., 2019; and  
650 the references therein). In turn, the deformation of rock glacier cores leads to the formation of networks of air voids and  
fractures, providing positive feedback on intra permafrost fluid flow.

The presence of liquid water in the rock glacier core is a prerequisite for the chemical interaction with the rock glacier  
sediments (Wanner et al., 2023a). Moreover, it introduces oxygen into the frozen core, promoting the oxidation of pyrite and  
655 thus the generation of sulfuric acid as the main weathering agent. If the amount of liquid water is limited and no fully  
connected water film can develop (Fig. 8a), the toxic elements mobilized from the sediments remain within the rock glacier  
and their concentrations in the rock glacier spring remain low. Owing to recurring cycles of freezing and thawing within the  
sediment ice mixture, with time this leads to a continuous enrichment and interim storage of the leached elements in the rock  
glacier ice. We hypothesize that this scenario is at play at high altitude or under colder climatic conditions than today, where  
660 the amount of ice in the rock glacier is stable. However, more research is required on how much time is needed to enrich  
toxic elements in rock glaciers However, more research is required on how much time for the enrichment of toxic elements  
in the rock glacier ice is needed to cause the high solute concentrations currently observed in the studied rock glacier springs.  
If the climatic conditions are too cold for seasonal temperatures at or above 0 °C, the rock glacier core is chemically inert,  
and the accumulation of elements pauses.

665 In the past years, climate warming likely led to an increase of in the time when the temperature at the top of the frozen core  
of the studied rock glacier is at or above zero. The same applies to the corresponding maximum temperature in summer.  
Consequently, the amount of liquid water increase<sub>d</sub>, and a fully connected water film has developed towards the top of the  
rock glacier core (i.e. the top of the sediment ice mixture) Such conditions, the. If water from snowmelt and precipitation  
670 events reaches the sediment ice mixture, intra permafrost flow becomes highly significant and the water film is exported

675 from the rock glacier system. We hypothesize that such hydraulic mobilization of the stagnant water film developed in response to climate warming is the main reason why the amount of water infiltrating into rock glaciers has such a strong control on the export of ice melt produced in the studied rock glacier. the 0 °C isotherm is near the surface (Williams et al., 2006) ice melt can happen. Furthermore, owing to the high heat capacity of water, the infiltration of water into the system brings thermal energy to the rock glacier core (Rist and Phillips, 2005; Williams et al., 2006), further promoting the degradation of the sediment ice matrix in addition to the hydraulic effect described above. This is particularly relevant under increased intra-permafrost flow, where the contact area between the ice and water is elevated.

### **5.2.3 Comparison with other conceptual models**

680 It should be noted that other studies have proposed that high concentrations of solutes in rock glacier springs are at least partly due to atmospheric deposition caused by industrial activities or volcanic eruption in addition to ARD (Nickus et al., 2023; Del Siro et al., 2023). Based on the very high solute fluxes currently exported from the studied rock glaciers only covering some 40000 m<sup>2</sup> (up to 10 t/a for trace solutes like Al and F<sup>-</sup>, see above), we consider such atmospheric sources not very likely for the studied system. This is consistent with other studies concluding that atmospheric deposition could be excluded as main cause for high solute concentrations in rock glacier springs (Thies et al., 2007; Steingruber et al., 2021).  
685 Moreover, a systematic monitoring of more than 150 rock glacier springs in Austria (Wagner et al., 2019) indicate that the enrichment of elements like Ni, Zn, Mn, Al, and sulfate occurs primarily in pragneissic geological settings but not in rock glacier draining other lithologies, which would likely be the case if atmospheric sources were relevant.

690 For the studied rock glacier in Val Costainas, the degradation of the rock glacier ice is significant enough to cause a disproportionally high discharge at the monitoring site AP5, located a few hundred meters downstream of the rock glacier (Table 1). Given that there are other rock glaciers in the Val Costainas catchment (Fig. 1a) and that the catchment is widely covered with other quaternary landforms such as talus, moraines, and alluvial cones characterized by significant water storage capacities (Arnoux et al., 2020, 2021), the strongly elevated discharge contribution at AP5 is quite remarkable. While it confirms the general potential of rock glaciers for subsurface water storage (Wagner et al., 2020; 2021b), it demonstrates  
695 that the rock glacier at the origin of Aua da Prasüra is currently very active hydraulically.

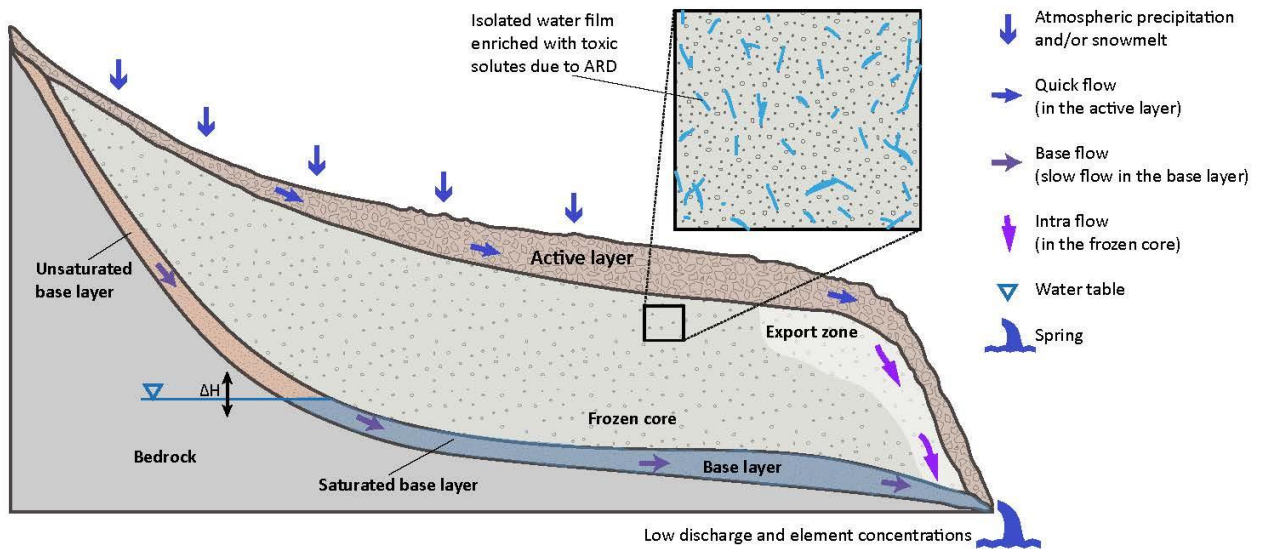
700 Since the frozen rock glacier core is likely heavily enriched with toxic elements, the coupled hydraulic thermal hydraulic degradation of the rock glacier ice is manifested by high concentrations in the lowest rock glacier spring AP1 (Fig. 5). In contrast, under dry conditions, the frozen rock glacier core is insulated from the hot summer temperatures at the surface (Hanson and Hoelzle, 2004; Humlum, 1997) and stagnant water films are protected from water driven export and their export is limited by gravity. As a consequence, under dry conditions the export of both ice melt and toxic elements remain rather low such as observed in 2022 (Figs. 7, 8).

The different modes for element enrichment and their subsequent mobilization (Fig. 8) reflect the variation of toxic element concentrations in the different rock glacier springs sampled in this study. The lowest concentrations are observed in the AP3 spring discharging at the highest elevation (2770 m a.s.l. Table 2). Here, the temperature is still too low to generate a continuous water film in late summer. Accordingly, the situation at this spring corresponds to that shown in Fig. 8a where export of ice melt, discharge and toxic element concentrations are low. With decreasing elevation, export of ice melt and hence the concentrations of toxic elements as well as the discharge strongly increase and the discharge may be significantly affected by ice melt. At the AP1 spring, located at an altitude of 2660 m a.s.l. (Figs. 1, 2) the situation corresponds to that shown in Fig. 8b and toxic element concentrations reach maximum values exceeding drinking water limits by factors of up to 226 (Table 2).

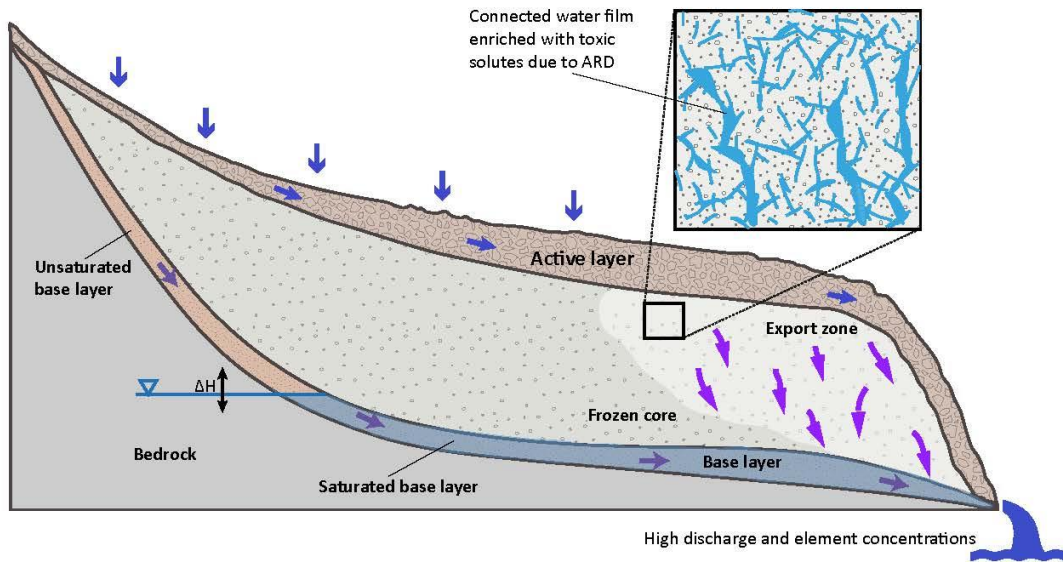
~~It should be noted that other studies have proposed that high concentrations of solutes in rock glacier springs are at least partly due to atmospheric deposition caused by industrial activities or volcanic degassing in addition to ARD (Nickus et al., 2023; Del Siro et al., 2023). Based on the very high solute fluxes currently exported from the studied rock glaciers only covering some 40000 m<sup>2</sup> (up to 10 t/a for trace elements like Al and F, see above), we consider such atmospheric sources not very likely for the studied system. This is consistent with other studies concluding that atmospheric deposition could be excluded as main cause for high solute concentrations in rock glacier springs (Thies et al., 2007; Steingruber et al., 2021). Moreover, a systematic monitoring of more than 150 rock glacier springs in Austria (Wagner et al., 2019) indicate that the enrichment of elements like Ni, Zn, Mn, Al, and sulfate occurs primarily in pragneissic geological settings but not in rock glacier draining other lithologies, which would likely be the case if atmospheric sources were relevant.~~



a) High altitude/colder climate than today: accumulation of elements



b) Current situation: degradation of ice and mobilization of elements



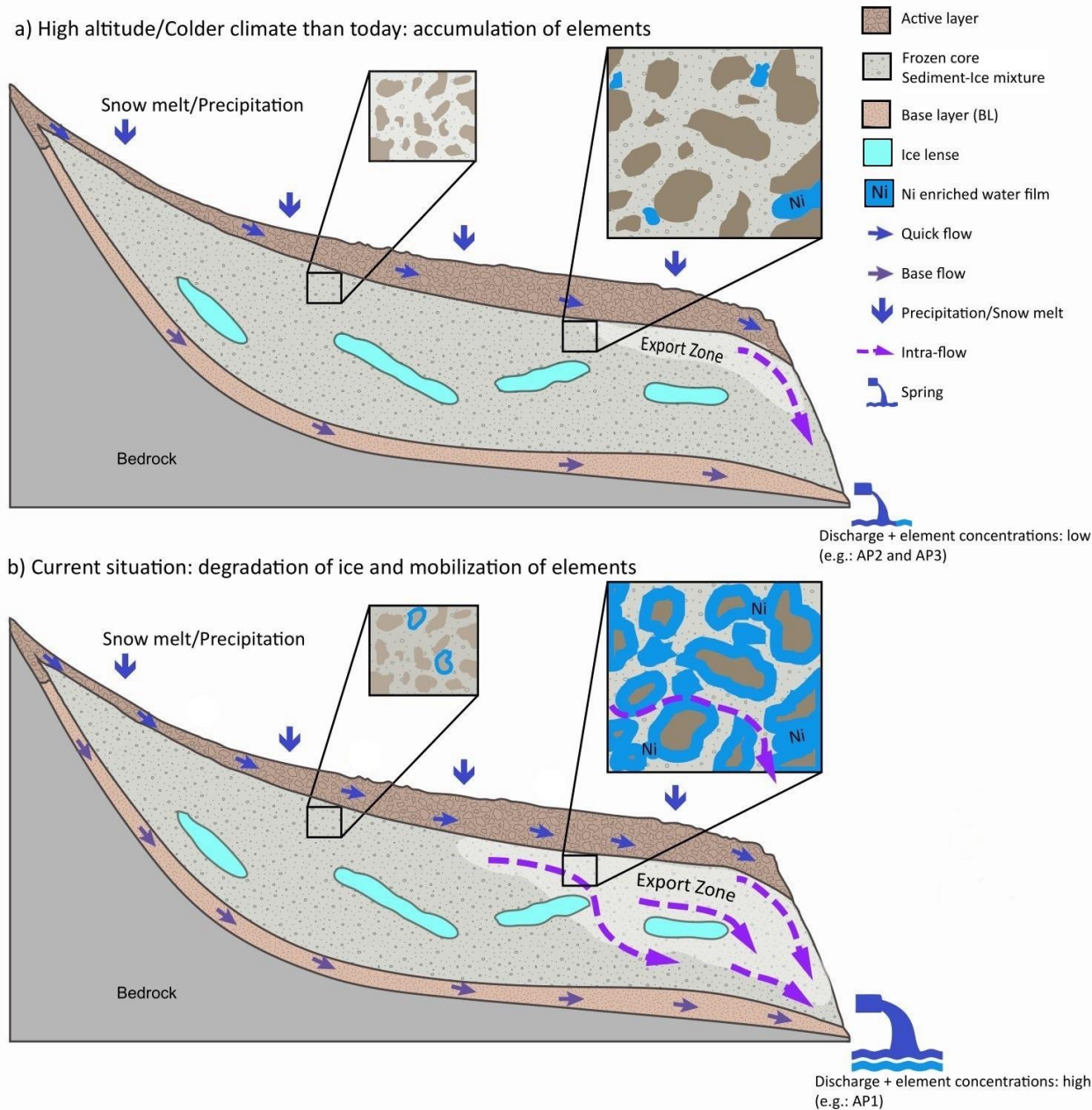


**Figure 8:** Conceptual schematic models of the coupled thermal-hydraulic-chemical processes controlling the mobilization of toxic solutes from intact rock glaciers affected by ARD. (a): Situation at high altitude or during climatic conditions where only small parts of the frozen rock glacier core (i.e. the sediment-ice mixture) are at or even above 0 °C in late summer. This leads to the formation of isolated and immobile water films from ice melt where chemical reactions with the host rock can occur. As a result of multiple seasonal freezing and thawing cycles, toxic solutes become enriched at the top of the rock glacier core and the amount of

730

735 ice in the rock glacier remains quasi-constant over time. (b): Situation during permafrost degradation such as today where a fully  
connected water film enriched in toxic solutes develops from ice melt in the front part of the rock glacier in late summer. This  
leads to a gravity-driven vertical export of both ice melt and toxic solutes to the unfrozen and water saturated base layer (export  
zone) where the residence time is up to several months. Hydraulic events such as snowmelt and rainfall increase the water table  
( $\Delta H$ ) in the base layer aquifer, causing the hydraulic export of water enriched in toxic solutes from the base layer. In late summer,  
740 rock glacier in Val Costainas, the coupled thermal-hydraulic degradation currently results in disproportionately high discharge  
(Table 1) and owing to the likely strong enrichment of solutes at the top of the rock glacier core, the flux of exported toxic solutes is  
up to several tons per year (Fig. 7).

### 5.3 Quantifying the export of ice melt from rock glaciers Environmental implications

745 The strong mobilization of toxic solutes (Ni, Mn, Al, and F<sup>-</sup>) from the studied rock glacier (Fig. 7) forms a hazard to the  
entire catchment shown in Figure 1. At the current export rates of up to several tons per year, the concentrations of Ni and  
Mn exceed the corresponding drinking water limits down to an altitude of about 1900 m a.s.l. during the entire summer  
season when the catchment is used for alpine livestock farming. As a consequence, the stream cannot be used as a drinking  
water source. Likewise, the quality of milk products from this farming may be affected because animals frequently drink  
from those affected stream. Moreover, the elevated concentrations of toxic solutes and low pH values not only degrade the  
750 downstream water quality; but may also cause significant ecological changes and disruptions in aquatic ecosystems (Thies et  
al., 2013; Ilyashuk et al., 2018). For instance, Ilyashuk et al. (2018) reported morphological deformities in some aquatic  
invertebrates due to ARD release into an alpine lake in South Tyrol, Italy. Similarly, the microbial diversity in close vicinity  
of the stream may be affected (Brighenti et al., 2019; Sannino et al., 2023). Based on our conceptual model (Fig. 8), the  
mobilization of toxic solutes will increase with accelerated permafrost degradation and toxic solute concentrations may  
755 further increase as well, until reaching a maximum at some point in the future. Owing to the high abundance of pyrite-  
bearing rocks, the same may apply to areas downstream of intact rock glaciers worldwide. Consequently, the water quality  
downstream of intact rock glaciers with pyrite-bearing rocks must be carefully monitored. Particularly important is to assess  
whether the mobilization of toxic solutes affects the water quality of larger streams in populated areas further downstream,  
acting as regional drinking water resources. At least for the European Alps, however, the risk for such regional  
760 contamination is considered limited. This is due to the spatially -limited, isolated occurrence of affected rock glaciers at high  
altitude above 2500 m a.s.l., which is far away from populated areas other than individual farms being operated during  
summer time.

765 In contrast to high-altitude systems, the environmental hazard caused by the degradation of ice-rich permafrost affected by  
ARD is likely much larger in high-latitude regions where permafrost occurs at low altitude and hence covers much larger  
areas. As recently shown for various sites in Alaska, the degradation of permafrost in regions with sulfide-bearing bedrock  
may decrease the water quality of large streams and thus forms a serious threat to the drinking water supply of local

770 communities as well as aquatic food webs including subsistence fisheries (O'Donnell et al., 2024). Given that the reported hazard in Alaska only started very recently, it is plausible that the water quality of the studied streams will further decline in the future and form a serious environmental hazard for a large area and a significant number of people. This is particularly the case if the mobilization of toxic solutes from high-latitude permafrost results from the previous accumulation of toxic solutes in the permafrost ice, such as postulated for the rock glacier in Val Costainas.

775 Although the environmental hazard caused by the mobilization of toxic solutes from rock glaciers in the European Alps may be limited, such mobilization could potentially serve as a novel environmental tracer to study permafrost degradation. This is because based on our conceptual model (Fig. 8), the fluxes of toxic solutes downstream of rock glaciers essentially reflect their final hydraulic mobilization from the solute-enriched rock glacier ice. Accordingly, all solutes must almost exclusively originate from their interim storage in the rock glacier ice. In contrast, their concentration in snowmelt and rainwater is negligible. It follows that monitoring toxic solute fluxes downstream of rock glaciers may allow to quantify the export of ice melt from rock glaciers. For instance, the observation that the annual fluxes of Ni and Zn exported from the studied rock glacier were 29-31 % lower in 2022 than in 2021 (Fig. 7) suggests that the export of ice melt followed a very similar pattern. This interpretation is remarkable given that 2022 corresponds to a year with record high temperatures in the Alps (Noetzi and Pellet, 2023), as manifested by much higher summer temperatures than in 2021 (Fig. S5). Moreover, it suggests that in our study area the variable infiltration of water into rock glaciers caused by a varying winter snow cover and variations in summer precipitation (Fig. 7) apparently has a much stronger effect on yearly ice melt export rates than the variation of the summer air temperature. To test the significance of toxic solutes fluxes as a novel permafrost degradation monitoring proxy, more research is required at selected test sites including long-term solute flux monitoring, the determination of solute concentrations in the frozen rock glacier cores, and the independent monitoring of rock glacier degradation by other (e.g., geophysical) methods.

790 ~~In addition to gaining novel insights into the coupled process controlling the export of ice melt from rock glaciers, the temporal storage of toxic solutes in rock glacier ice may allow to quantify the actual export of ice melt. While the relative changes of mobilized fluxes directly correspond to the relative changes in the export rates, the estimation of absolute values is more challenging. It is only possible if the following two conditions are met, (i) occurrence of constant concentrations of the enriched elements in the rock glacier ice, and (ii) knowledge about their actual concentrations in the rock glacier ice. If both conditions are met, the ice melt contribution at downstream sampling locations can be estimated based on seasonal concentration curves such as shown in Fig. 8a,b using a binary mixing model:~~

$$795 \text{ Ice melt contribution (\%)} = (X_f / X_{\text{endmember}}) * 100 \quad (2)$$

$$800 \text{ Ice melt (L s}^{-1}\text{)} = \text{Ice melt contribution} * Q_i \quad (3)$$

Where  $X_t$  is the concentration of the solute of interest at time  $t$  ( $\text{mg L}^{-1}$ ),  $X_{\text{endmember}}$  is the concentration of the solute in the ice (the endmember), and  $Q_t$  is the discharge at time  $t$ .

805 While determining the concentration of elements in rock glacier ice feasible by drilling into these landforms and subsequently analyzing the melted ice (Nickus et al., 2023), the prerequisite of having constant concentration in the ice is unlikely to be met. In fact, Nickus et al. (2023) have shown that there are rather strong variations of toxic element concentrations along the frozen core retrieved from the Lazaun rock glacier. Nevertheless, the highest concentrations were observed towards the top of the sediment ice mixture where the temperature is seasonally at or even above  $0^\circ\text{C}$ . According to the conceptual model, this is exactly the location where most of the ice melt export occurs (i.e. the Export Zone as shown in Fig. 10). Accordingly, determining the average element concentrations in this uppermost part of frozen rock glacier cores might be representative for the element concentration of the meltwater. Therefore, these concentrations could be used for obtaining meaningful estimates of the amount of ice melt being exported from rock glaciers based on toxic solute concentrations continuously measured in the downhill streams.

815 To test the proposed approach for the studied system, we took the seasonal variation of the concentrations of Ni and Zn at AP10 (Fig. 5). In the absence of drillcores, we further estimated the concentration of both elements in the rock glacier ice by taking their highest concentration measured at the AP1 rock glacier spring (Fig. 1), which are  $3.3$  and  $7.8 \text{ mg L}^{-1}$ , respectively. This resulted in the seasonal ice melt export curves shown in Fig. 11. For the May to October monitoring period in 2021, integrating these curves resulted in a total export of ice melt of  $283'676 \text{ m}^3$  based on Ni and  $326'586 \text{ m}^3$  for Zn. For 2022, the integration resulted in a total export of  $195'425 \text{ m}^3$  based on Ni and  $234'635 \text{ m}^3$  based on Zn.

825 We consider the fact that similar ice melt export rates are obtained for a specific monitoring year when using different elements for the quantification (2021:  $\pm 15\%$ ; 2022:  $\pm 17\%$ ) as a proof of concept that the proposed approach works. The same applies for the observation that the relative variation of the estimated ice melt export rates between the two monitoring years is very similar than the variation of the corresponding annual element fluxes (both ca.  $30\%$  lower in 2022 than in 2021, *c.f.* Figs. 8a,b). It follows that tracking element fluxes downstream of intact rock glaciers allows obtaining reliable estimates of the relative variation of ice melt export rates without knowing the concentration of the elements in the rock glacier ice.

835 In contrast, the estimated amounts of total ice melt exported from the studied rock glacier per monitoring period (Fig. 11) are strongly overestimated because the concentrations in AP1 are certainly lower than the maximum concentration in the rock glacier ice. This is manifested by relating the estimated export rates to the surface area of the studied rock glacier ( $40'000$

m<sup>2</sup>). In the two monitoring years, the average yearly export of ice melt obtained from the two elements correspond to a degradation of 7.5 (2021) and 5.3 m (2022). Considering that Krainer et al. (2015) estimated an annual rock glacier ice degradation of about 10 centimeters, our estimates are at least one order of magnitude too high. The overestimation likely reflects the degree of dilution between the rock glacier ice and API. This is consistent with data from the Lazaun rock glacier ice, where the concentrations of Ni, and Zn in the rock glacier ice are about 10 times higher than in the corresponding rock glacier spring (Nickus et al., 2023). This confirms that reliable estimates may be obtained when drilling into the rock glacier and determining the concentrations of elements enriched in the rock glacier ice.

Overall, our data demonstrate the great potential of the strong chemical signal observed in springs discharging from intact rock glaciers affected by ARD to continuously track the relative and maybe even the absolute amounts of ice melt exported from rock glaciers. Installing multiple monitoring stations at different rock glaciers could thus help to obtain more insights on regional and maybe even global ice melt export rates in rock glacier systems. In a first step, such effort should focus on systems affected by ARD because of their strong chemical signal, which allow estimating the fluxes at distant downstream locations more accessible for continuous sampling and measurements than the actual rock glacier springs. Future research, however, should also focus on systems not affected by ARD in order to assess whether an enrichment of solutes in ice is also detectable in chemically less reactive systems and subsequently used for quantifying the export of ice melt.

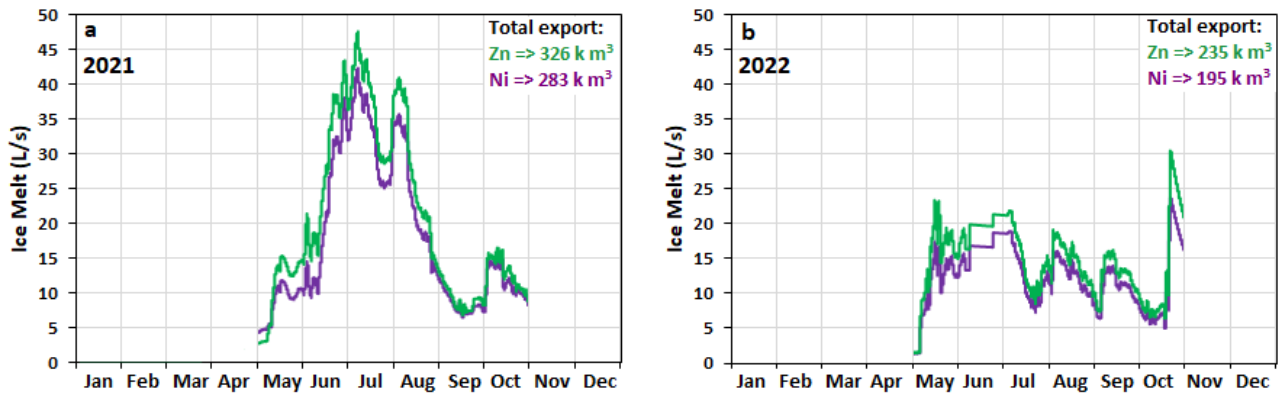


**Figure 11: Estimates of seasonal evolution of ice melt exported from the rock glacier at the origin of Aua da Prasiira estimated based on the fluxes of Ni and Zn at AP10 and the corresponding maximum concentrations in the rock glacier spring at AP1. (a) 2021, (b) 2022.**

## 6 Conclusions

860 The detailed, two-year long monitoring of a high-alpine stream affected by acid rock drainage (ARD) in Eastern Switzerland provided novel insights into the causes for the massive mobilization of toxic solutes such as Al, F<sup>-</sup>, Zn, Mn, and Ni ~~from an intact rock glacier located at the origin of the stream~~. The main conclusions and implications ~~for the future~~ are listed below:

865 - Compared to concentration measurements, tracking of solute fluxes were more important for increasing our understanding of the mobilization process. This is because, unlike solute fluxes, solute concentrations are influenced by dilution from snowmelt and atmospheric precipitation.

870 - In the studied catchment, the majority of the toxic solutes is mobilized from an intact rock glacier at the origin of the stream. As a consequence, in the rock glaciers springs their concentrations exceeding drinking water limits by factors of up to 226. At 5 km downstream, ~~these concentrations still exceed the~~ drinking water limits are still exceeded by factors of up to 15. The corresponding fluxes are on the order of several tons per year, which is remarkable given that the surface area of the studied rock glacier only covers an area of around 40000 m<sup>2</sup>. ~~the fluxes of these solutes are remarkably high, reaching up to several tons per year~~ Furthermore, the high fluxes demonstrate that intact rock glaciers may act as very strong chemical reactors.

875 - The presence of liquid water in the rock glacier core is required for the production of sulfuric acid as a weathering agent, promoting the dissolution of the toxic solutes from the host rock. Moreover, it introduces oxygen, accelerating pyrite weathering. In the past, recurring cycles of freezing and thawing within the sediment-ice mixture (i.e. the rock glacier core), have led to the enrichment and interim storage of the leached solutes in the rock glacier ice. Hence, the presented data fully verified the initial storage and enrichment hypothesis of Wanner et al. (2023).

880 - Today, climate warming increases the temperature of the top of the frozen core, causing the formation of a continuous water film enriched in toxic solutes at the interface between sediments and ice in late summer. Infiltration of water from snowmelt and precipitation leads to a quick hydraulic export ~~of the water film from the rock glacier causing export~~ of both ice melt and toxic solutes. This is manifested by the strong positive correlation between solutes fluxes and the discharge.

885 - In the studied system, the export of ice melt from the rock glaciers currently causes a disproportionately high discharge in summer, confirming that rock glaciers will play a more important role as water resources in alpine regions.

890 - The fluxes of toxic ~~solute~~ elements exported from intact rock glaciers affected by ARD are likely to increase until reaching a maximum. More research is required to estimate when this will be reached and what the maximum concentrations and fluxes will be. This increase in the ~~toxic element~~ concentration of toxic solutes corresponds to a decline in water quality downstream of rock glaciers impacted by ARD, emphasizing the necessity for continuous monitoring of such systems. In high-altitude settings such as in the Central Eastern Alps, however, the risk for

larger streams in populated areas further downstream is considered limited. This is due to the spatially limited, isolated occurrence of affected rock glaciers at high altitude above 2500 m a.s.l., which is far away from populated areas other than individual farms being operated during summer time. In contrast, the environmental hazard caused by the degradation of ice-rich permafrost affected by ARD is likely much larger in high-latitude regions where permafrost covers much larger areas.

- As the fluxes of toxic solutes downstream of rock glaciers essentially reflect their final hydraulic mobilization from the rock solute-enriched rock glacier ice, flux measurements may serve as a novel environmental tracer to study permafrost degradation.

This strong chemical signal provides the opportunity to quantify the amount of ice melt exported from rock glaciers. Our data demonstrate that relative changes in element fluxes correspond to relative changes in the export rates of ice melt. Moreover, it demonstrates that determining the absolute export rates of ice melt would be feasible if the concentrations of solutes in the rock glacier ice were known. Consequently, monitoring solute fluxes exported from rock glaciers is a promising future research direction for obtaining more reliable estimates of the amount ice melt exported from rock glaciers.

### **Data availability**

Research data can be accessed at <https://zenodo.org/doi/10.5281/zenodo.10558549> (Moradi et al., 2024).

### **Author contribution**

HM and CW designed the study. HM, CW, GF, and MM carried out the sampling and monitoring campaigns. HM, performed the chemical analyses of streamwater. HM and CW analyzed the data. HM with supervision of CW wrote the original draft. DM planned the UAV survey and prepared the figures showing maps. CW, GF, DM, and MM reviewed and edited the draft. CW acquired funding and was responsible for project management.

### **Competing interests**

The contact author has declared that none of the authors has any competing interests.

### **Acknowledgements**

We express our gratitude to Priska Bähler, Philipp Hänggi, and Christopher Pichler for their support in the chemical analyses of streamwater. Special appreciation goes to Linda Feichtinger and her team from Biosfera Val Müstair for their dedicated



920 efforts in conducting bi-weekly water sampling. We also thank Marco Ferrari and David Schmid from the Amt für Natur und  
Umwelt, Canton of Graubünden (ANU) for maintaining the combined water table and electric conductivity probe used in  
this study.

### Financial support

This research was funded by the Swiss National Science Foundation, which is greatly appreciated (SNSF Grant 196847 to  
CW).

### 925 References

- ANU:  
[https://www.gr.ch/DE/institutionen/verwaltung/ekud/anu/aktuelles/umweltbeobachtung/hydrodaten/Seiten/Hydrodaten.aspx  
#/device/UMBRAIL\\_20/pegel\\_m](https://www.gr.ch/DE/institutionen/verwaltung/ekud/anu/aktuelles/umweltbeobachtung/hydrodaten/Seiten/Hydrodaten.aspx#/device/UMBRAIL_20/pegel_m), last access: 11 January 2024.
- Ballantyne, C. K.: Periglacial Geomorphology, John Wiley & Sons Ltd, 2018.
- 930 Barsch, D.: Rockglaciers, Springer Berlin Heidelberg, Berlin, Heidelberg, 331 pp., <https://doi.org/10.1007/978-3-642-80093-1>, 1996.
- Brighenti, S., Tolotti, M., Bruno, M. C., Wharton, G., Pusch, M. T., and Bertoldi, W.: Ecosystem shifts in Alpine streams under glacier retreat and rock glacier thaw: A review, *Sci. Total Environ.*, 675, 542–559, <https://doi.org/10.1016/j.scitotenv.2019.04.221>, 2019.
- 935 Brighenti, S., Engel, M., Tolotti, M., Bruno, M. C., Wharton, G., Comiti, F., Tirler, W., Cerasino, L., and Bertoldi, W.: Contrasting physical and chemical conditions of two rock glacier springs, *Hydrol. Process.*, 35, 1–18, <https://doi.org/10.1002/hyp.14159>, 2021.
- Calkins, D. and Dunne, T.: A salt tracing method for measuring channel velocities in small mountain streams, *J. Hydrol.*, 11, 379–392, [https://doi.org/https://doi.org/10.1016/0022-1694\(70\)90003-X](https://doi.org/https://doi.org/10.1016/0022-1694(70)90003-X), 1970.
- 940 Colombo, N., Gruber, S., Martin, M., Malandrino, M., Magnani, A., Godone, D., Freppaz, M., Fratianni, S., and Salerno, F.: Rainfall as primary driver of discharge and solute export from rock glaciers: The Col d’Olen Rock Glacier in the NW Italian Alps, *Sci. Total Environ.*, 639, 316–330, <https://doi.org/10.1016/j.scitotenv.2018.05.098>, 2018.
- Day, T. J.: Observed mixing lengths in mountain streams, *J. Hydrol.*, 35, 125–136, [https://doi.org/https://doi.org/10.1016/0022-1694\(77\)90081-6](https://doi.org/https://doi.org/10.1016/0022-1694(77)90081-6), 1977.
- 945 Diem, D. and Stumm, W.: Is dissolved Mn<sup>2+</sup> being oxidized by O<sub>2</sub> in absence of Mn-bacteria or surface catalysts?, *Geochim. Cosmochim. Acta*, 48, 1571–1573, [https://doi.org/https://doi.org/10.1016/0016-7037\(84\)90413-7](https://doi.org/https://doi.org/10.1016/0016-7037(84)90413-7), 1984.
- Dold, B., Aguilera, a, Cisternas, M. E., Bucchi, F., and Amils, R.: Sources for Iron Cycling in the Southern Ocean, *Environ. Sci. Technol.*, 47, 6129–6136, 2013.
- 950 Exley, C.: The toxicity of aluminium in humans., *Morphologie*, 100, 51–55, <https://doi.org/10.1016/j.morpho.2015.12.003>, 2016.
- Fortner, S. K., Mark, B. G., McKenzie, J. M., Bury, J., Trierweiler, A., Baraer, M., Burns, P. J., and Munk, L. A.: Elevated stream trace and minor element concentrations in the foreland of receding tropical glaciers, *Appl. Geochemistry*, 26, 1792–1801, <https://doi.org/10.1016/j.apgeochem.2011.06.003>, 2011.
- Giardino, J. R. and Vitek, J. D.: The significance of rock glaciers in the glacial-periglacial landscape continuum, *J. Quat.*

- 955 Sci., 3, 97–103, <https://doi.org/https://doi.org/10.1002/jqs.3390030111>, 1988.
- Giardino John R, Vitek John D, D. J. L.: Periglacial Geomorphology, in: A Model of Water Movement in Rock Glaciers and Associated Water Characteristics, 26, <https://doi.org/https://doi.org/10.4324/9781003028901>, 1992.
- Haeberli, W.: Creep of mountain permafrost: internal structure and flow of alpine rock glaciers, *Mitteilungen der Versuchsanstalt für Wasserbau, Hydrol. und Glaziologie an der Eidgenoss. Tech. Hochschule Zurich*, 1985.
- 960 Harrington, J. S., Mozil, A., Hayashi, M., and Bentley, L. R.: Groundwater flow and storage processes in an inactive rock glacier, *Hydrol. Process.*, 32, 3070–3088, <https://doi.org/10.1002/hyp.13248>, 2018.
- Hayashi, M.: Alpine Hydrogeology: The Critical Role of Groundwater in Sourcing the Headwaters of the World, *Groundwater*, 58, 498–510, <https://doi.org/10.1111/gwat.12965>, 2020.
- 965 Humlum, O.: Active layer thermal regime at three rock glaciers in Greenland, *Permafrost and Periglacial Processes*, 8, 383–408, [https://doi.org/10.1002/\(SICI\)1099-1530\(199710/12\)8:4<383::AID-PPP265>3.0.CO;2-V](https://doi.org/10.1002/(SICI)1099-1530(199710/12)8:4<383::AID-PPP265>3.0.CO;2-V), 1997.
- Ilyashuk, B. P., Ilyashuk, E. A., Psenner, R., Tessadri, R., and Koinig, K. A.: Rock glacier outflows may adversely affect lakes: Lessons from the past and present of two neighboring water bodies in a crystalline-rock watershed, *Environ. Sci. Technol.*, 48, 6192–6200, <https://doi.org/10.1021/es500180c>, 2014.
- 970 Ilyashuk, B. P., Ilyashuk, E. A., Psenner, R., Tessadri, R., and Koinig, K. A.: Rock glaciers in crystalline catchments: Hidden permafrost-related threats to alpine headwater lakes, *Glob. Chang. Biol.*, 24, 1548–1562, <https://doi.org/10.1111/gcb.13985>, 2018.
- Jones, D. B., Harrison, S., Anderson, K., and Betts, R. A.: Mountain rock glaciers contain globally significant water stores, *Sci. Rep.*, 8, 1–10, <https://doi.org/10.1038/s41598-018-21244-w>, 2018.
- 975 Jones, D. B., Harrison, S., Anderson, K., and Whalley, W. B.: Rock glaciers and mountain hydrology: A review, *Earth-Science Reviews*, 193, 66–90, <https://doi.org/10.1016/j.earscirev.2019.04.001>, 2019.
- Kenner, R., Noetzli, J., Hoelzle, M., Raetzo, H., and Phillips, M.: Distinguishing ice-rich and ice-poor permafrost to map ground temperatures and ground ice occurrence in the Swiss Alps, *Cryosphere*, 13, 1925–1941, <https://doi.org/10.5194/tc-13-1925-2019>, 2019.
- 980 Krainer, K. and Mostler, W.: Hydrology of Active Rock Glaciers: Examples from the Austrian Alps, Arctic, Antarctic, *Alp. Res.*, 34, 142–149, <https://doi.org/10.1080/15230430.2002.12003478>, 2002.
- Krainer, K., Mostler, W., and Spötl, C.: Discharge from active rock glaciers, Austrian Alps: A stable isotope approach, *Austrian J. Earth Sci.*, 100, 102–112, 2007.
- 985 Krainer, K., Bressan, D., Dietre, B., Haas, J. N., Hajdas, I., Lang, K., Mair, V., Nickus, U., Reidl, D., Thies, H., and Tonidandel, D.: A 10,300-year-old permafrost core from the active rock glacier Lazaun, southern Ötztal Alps (South Tyrol, northern Italy), *Quat. Res. (United States)*, 83, 324–335, <https://doi.org/10.1016/j.yqres.2014.12.005>, 2015.
- Leibundgut, C., Maloszewski, P., and Külls, C.: Tracers in Hydrology, *Tracers Hydrol.*, 1–415, <https://doi.org/10.1002/9780470747148>, 2009.
- Li, M., Yang, Y., Peng, Z., and Liu, G.: Assessment of rock glaciers and their water storage in Guokalariju, Tibetan Plateau, *Cryosphere*, 18, 1–16, <https://doi.org/10.5194/tc-18-1-2024>, 2024.
- 990 MeteoSwiss: <https://www.meteoschweiz.admin.ch/service-und-publikationen/applikationen/messwerte-und-messnetze.html#lang=de&swisstopoApiKey=cpZJOL3HuO5yENksi97q&param=messwerte-niederschlag-10min&station=SMM&chart=month>, last access: 11 January 2024.
- 995 Moradi, H., Furrer, G., Michael, M., David, M., and Wanner, C.: Massive mobilization of toxic elements from an intact rock glacier in the Central Eastern Alps: insights on ice melt dynamics, <https://doi.org/https://zenodo.org/doi/10.5281/zenodo.10558549>, 2024.
- Muniz, I. P.: Freshwater acidification: its effects on species and communities of freshwater microbes, plants and animals, *Proc. R. Soc. B Biol. Sci.*, 97, 227–254, 1990.

- Munroe, J. S. and Handwerger, A. L.: Contribution of rock glacier discharge to late summer and fall streamflow in the Uinta Mountains, Utah, USA, *Hydrol. Earth Syst. Sci.*, 27, 543–557, <https://doi.org/10.5194/hess-27-543-2023>, 2023.
- 1000 Nickus, U., Thies, H., Krainer, K., Lang, K., Mair, V., and Tonidandel, D.: A multi-millennial record of rock glacier ice chemistry (Lazaun, Italy), *Front. Earth Sci.*, 11, <https://doi.org/10.3389/feart.2023.1141379>, 2023.
- Noetzli, J. and Pellet, C. (eds. : PERMOS, Swiss Permafrost Bulletin 2022, 23 pp., <https://doi.org/Available at: https://www.permos.ch/publications>, 2023.
- O'Donnell, J. A., Carey, M. P., Koch, J. C., Baughman, C., Hill, K., Zimmerman, C. E., Sullivan, P. F., Dial, R., Lyons, T., 1005 Cooper, D. J., and Poulin, B. A.: Metal mobilization from thawing permafrost to aquatic ecosystems is driving rusting of Arctic streams, *Commun. Earth Environ.*, 5, <https://doi.org/10.1038/s43247-024-01446-z>, 2024.
- Rist, A. and Phillips, M.: First results of investigations on hydrothermal processes within the active layer above alpine permafrost in steep terrain, *Nor. Geogr. Tidsskr.*, 59, 177–183, <https://doi.org/10.1080/00291950510020574>, 2005.
- 1010 Sannino, C., Qi, W., Rütli, J., Stierli, B., and Frey, B.: Distinct taxonomic and functional profiles of high Arctic and alpine permafrost-affected soil microbiomes, *Environ. Microbiome*, 18, 1–22, <https://doi.org/10.1186/s40793-023-00509-6>, 2023.
- Schmid, S. M., Fügenschuh, B., Kissling, E., and Schuster, R.: Tectonic map and overall architecture of the Alpine orogen, *Eclogae Geol. Helv.*, 97, 93–117, <https://doi.org/10.1007/s00015-004-1113-x>, 2004.
- Schmid, S. V.: *Geologie des Umbrailgebiets*, 66, 101–210, <https://doi.org/http://dx.doi.org/10.5169/seals-164185>, 1973.
- 1015 Shaw, C. A. and Tomljenovic, L.: Aluminum in the central nervous system (CNS): toxicity in humans and animals, vaccine adjuvants, and autoimmunity., *Immunol. Res.*, 56, 304–316, <https://doi.org/10.1007/s12026-013-8403-1>, 2013.
- Del Siro, C., Scapozza, C., Perga, M. E., and Lambiel, C.: Investigating the origin of solutes in rock glacier springs in the Swiss Alps: A conceptual model, *Front. Earth Sci.*, 11, 1–20, <https://doi.org/10.3389/feart.2023.1056305>, 2023.
- SLF: <https://www.slf.ch/de/lawinenbulletin-und-schneesituation/messwerte/beschreibung-automatische-stationen/>, last access: 11 January 2024.
- 1020 Steingruber, S. M., Bernasconi, S. M., and Valenti, G.: Climate Change-Induced Changes in the Chemistry of a High-Altitude Mountain Lake in the Central Alps, *Aquat. Geochemistry*, 27, 105–126, <https://doi.org/10.1007/s10498-020-09388-6>, 2021.
- Swisstopo: <https://shop.swisstopo.admin.ch/en/maps/geological-maps/explanatory-booklet-geological-atlas-switzerland-25000>, last access: 11 January 2024a.
- 1025 Swisstopo: <https://www.swisstopo.admin.ch/en/geodata/geology/maps/geocover.html>, last access: 11 January 2024b.
- Tenthorey, G.: Perennial névés and the hydrology of rock glaciers, *Permafr. Periglac. Process.*, 3, 247–252, <https://doi.org/10.1002/ppp.3430030313>, 1992.
- Thies, H., Nickus, U., Mair, V., Tessadri, R., Tait, D., Thaler, B., and Psenner, R.: Unexpected response of high alpine lake waters to climate warming, *Environ. Sci. Technol.*, 41, 7424–7429, <https://doi.org/10.1021/es0708060>, 2007.
- 1030 Thies, H., Nickus, U., Tolotti, M., Tessadri, R., and Krainer, K.: Evidence of rock glacier melt impacts on water chemistry and diatoms in high mountain streams, *Cold Reg. Sci. Technol.*, 96, 77–85, <https://doi.org/10.1016/j.coldregions.2013.06.006>, 2013.
- Thies, H., Nickus, U., Tessadri, R., Tropper, P., and Krainer, K.: Peculiar arsenic, copper, nickel, uranium, and yttrium-rich stone coatings in a high mountain stream in the Austrian alps, *Austrian J. Earth Sci.*, 110, 1035 <https://doi.org/10.17738/ajes.2017.0012>, 2017.
- Todd, A. S., Manning, A. H., Verplanck, P. L., Crouch, C., McKnight, D. M., and Dunham, R.: Climate-change-driven deterioration of water quality in a mineralized watershed, *Environ. Sci. Technol.*, 46, 9324–9332, <https://doi.org/10.1021/es3020056>, 2012.
- Vergilio, C. dos S., Lacerda, D., da Silva Souza, T., de Oliveira, B. C. V., Fioresi, V. S., de Souza, V. V., da Rocha

- 1040 Rodrigues, G., de Araujo Moreira Barbosa, M. K., Sartori, E., Rangel, T. P., de Almeida, D. Q. R., de Almeida, M. G., Thompson, F., and de Rezende, C. E.: Immediate and long-term impacts of one of the worst mining tailing dam failure worldwide (Bento Rodrigues, Minas Gerais, Brazil), *Sci. Total Environ.*, 756, <https://doi.org/10.1016/j.scitotenv.2020.143697>, 2021.
- 1045 Wagner, T., Kainz, S., Wedenig, M., Pleschberger, R., Krainer, K., Kellerer-Pirklbauer, A., Ribis, M., Hergarten, S., and Winkler, G.: *Wasserwirtschaftliche Aspekte von Blockgletschern in Kristallingebieten der Ostalpen*, 2019.
- Wagner, T., Brodacz, A., Krainer, K., and Winkler, G.: Active rock glaciers as shallow groundwater reservoirs, *Austrian Alps, Grundwasser*, 25, 215–230, <https://doi.org/10.1007/s00767-020-00455-x>, 2020.
- 1050 Wagner, T., Seelig, S., Helfricht, K., Fischer, A., Avian, M., Krainer, K., and Winkler, G.: Assessment of liquid and solid water storage in rock glaciers versus glacier ice in the Austrian Alps, *Sci. Total Environ.*, 800, 149593, <https://doi.org/10.1016/j.scitotenv.2021.149593>, 2021a.
- Wagner, T., Kainz, S., Krainer, K., and Winkler, G.: Storage-discharge characteristics of an active rock glacier catchment in the Innere Ölgrube, *Austrian Alps, Hydrol. Process.*, 35, 1–16, <https://doi.org/10.1002/hyp.14210>, 2021b.
- 1055 Wanner, C., Pöthig, R., Carrero, S., Fernandez-Martinez, A., Jäger, C., and Furrer, G.: Natural occurrence of nanocrystalline Al-hydroxysulfates: Insights on formation, Al solubility control and As retention, *Geochim. Cosmochim. Acta*, 238, 252–269, <https://doi.org/10.1016/j.gca.2018.06.031>, 2018.
- Wanner, C., Moradi, H., Ingold, P., Cardenas Bocanegra, M. A., Mercurio, R., and Furrer, G.: Rock glaciers in the Central Eastern Alps – How permafrost degradation can cause acid rock drainage, mobilization of toxic elements and formation of basaluminite, *Glob. Planet. Change*, 227, <https://doi.org/10.1016/j.gloplacha.2023.104180>, 2023.
- 1060 Williams, M. W., Knauf, M., Caine, N., Liu, F., and Verplanck, P. L.: Geochemistry and source waters of rock glacier outflow, *Colorado Front Range, Permafr. Periglac. Process.*, 17, 13–33, <https://doi.org/10.1002/ppp.535>, 2006.
- Williamson, M. A. and Rimstidt, J. D.: The kinetics and electrochemical rate-determining step of aqueous pyrite oxidation, *Geochim. Cosmochim. Acta*, 58, 5443–5454, [https://doi.org/https://doi.org/10.1016/0016-7037\(94\)90241-0](https://doi.org/https://doi.org/10.1016/0016-7037(94)90241-0), 1994.
- Zarroca, M., Roqué, C., Linares, R., Salminci, J. G., and Gutiérrez, F.: Natural acid rock drainage in alpine catchments: A side effect of climate warming, *Sci. Total Environ.*, 778, 146070, <https://doi.org/10.1016/j.scitotenv.2021.146070>, 2021.
- 1065